



Universiteit
Leiden
The Netherlands

Oxidative stress in experimental bronchopulmonary dysplasia

Horst, S.A.J. ter

Citation

Horst, S. A. J. ter. (2008, June 12). *Oxidative stress in experimental bronchopulmonary dysplasia*. Retrieved from <https://hdl.handle.net/1887/12949>

Version: Corrected Publisher's Version

License: [Licence agreement concerning inclusion of doctoral thesis in the Institutional Repository of the University of Leiden](#)

Downloaded from: <https://hdl.handle.net/1887/12949>

Note: To cite this publication please use the final published version (if applicable).

Chapter

2

**Gene expression profile and
histopathology of experimental
bronchopulmonary dysplasia induced
by prolonged oxidative stress**

Gene expression profile and histopathology of experimental bronchopulmonary dysplasia induced by prolonged oxidative stress

Gerry T.M. Wagenaar
Simone A.J. ter Horst
Margôt A. van Gastelen
Lara M. Leijser
Thais Mauad
Pieter A. van der Velden
Emile de Heer
Pieter S. Hiemstra
Ben J.H.M. Poorthuis
Frans J. Walther

Free Radic Biol Med 36(6):782-801, 2004

ABSTRACT

Oxidative stress is an important factor in the pathogenesis of bronchopulmonary dysplasia (BPD), a chronic lung disease of premature infants characterized by arrested alveolar and vascular development of the immature lung. We investigated differential gene expression with DNA microarray analysis in premature rat lungs exposed to prolonged hyperoxia during the sacular stage of development, which closely resembles the development of the lungs of premature infants receiving neonatal intensive care. Expression profiles were largely confirmed by real-time RT-PCR (27 genes) and in line with histopathology and fibrin deposition studied by Western blotting. Oxidative stress affected a complex orchestra of genes involved in inflammation, coagulation, fibrinolysis, extracellular matrix turnover, cell cycle, signal transduction, and alveolar enlargement and explains, at least in part, the pathological alterations that occur in lungs developing BPD. Exciting findings were the magnitude of fibrin deposition; the upregulation of chemokine-induced neutrophilic chemoattractant-1 (CINC-1), monocyte chemoattractant protein-1 (MCP-1), amphiregulin, plasminogen activator inhibitor-1 (PAI-1), secretory leukocyte proteinase inhibitor (SLPI), matrix metalloproteinase-12 (MMP12), p21, metallothionein, and heme oxygenase (HO); and the downregulation of fibroblast growth factor receptor-4 (FGFR4) and vascular endothelial growth factor (VEGF) receptor-2 (Flk-1). These findings are not only of fundamental importance in the understanding of the pathophysiology of BPD, but also essential for the development of new therapeutic strategies.

INTRODUCTION

Neonatal intensive care has been increasingly effective in reducing the mortality of very premature infants at the expense of an increasing number of survivors with bronchopulmonary dysplasia (BPD). BPD is a chronic lung disease that develops in newborn infants treated with oxygen and positive pressure ventilation for respiratory distress. Infants with BPD, defined clinically by a continuing need for oxygen supplementation at 36 weeks postmenstrual age, are at high risk for morbidity and mortality during the first years of life and many of them have respiratory problems throughout childhood and young adulthood (35). BPD is particularly seen in infants born at less than 30 weeks of gestation and with a birth weight less than 1200 g (3, 29). At birth the lungs of these infants are underdeveloped, surfactant-deficient, fluid-filled, and not supported by a stiff chest wall, which enhances their susceptibility to lung injury and inflammation (29). Oxidative stress plays an important role in the development of BPD, which is characterized by decreased alveolarization and vascularization of the developing lung (29, 30).

Animal models of BPD are critical for characterizing the pathophysiology of BPD and testing of potential treatment options (30). Exposure of premature baboons (10), neonatal mice (7, 53), and rats (9, 23, 45) to hyperoxia results in progressive lung disease, which strongly resembles BPD in premature infants. Although a recent NHLBI Workshop proposed differential gene expression in uninjured and injured lungs as a research priority to learn how inflammation and injury are expressed by the developing lung (30), gene expression profiles of BPD in premature infants are still lacking. Therefore, we investigated histopathology and differential gene expression in experimental BPD using DNA microarray technology and real-time RT-PCR in a premature rat model with chronic lung injury, induced by prolonged exposure to hyperoxia, and demonstrate the significance of this model for studying BPD in premature infants.

MATERIALS AND METHODS

Animals. Timed-pregnant Wistar rats were kept in a 12 h dark/light cycle and fed a standard chow diet (Special Diet Services, Witham, Essex, England) ad libitum. Animal care was in accordance with institutional guidelines of the Leiden University Medical Center. Spontaneous birth occurred 22 days after conception. After a gestation of 21 days, pregnant rats were killed by decapitation and pups were delivered by hysterectomy through a median abdominal incision. Immediately after birth, the premature rat pups were dried and stimulated. Pups of three litters were pooled and randomly distributed over three groups: an oxygen (O₂) group and two room air (RA) groups, of which the RA1 group was the control. Litter size was 14

pups per litter in the oxygen and RA1 group and 5 pups in the RA2 group. Pups were fed by lactating foster dams, which were rotated daily to avoid oxygen toxicity. Foster dams were exposed to 100% oxygen for 24 h at 72 h intervals and to room air for 48 h. Pups were kept up to 14 days in transparent 50 x 50 x 70 cm Plexiglass chambers and exposed to 100% oxygen or room air. The oxygen concentration in the chamber was monitored daily with an oxygen sensor (Drägerwerk AG, Lübeck, Germany) and maintained at 100% with a flow of 5 L of oxygen/min. Body weight of the pups was measured daily.

Tissue preparation. After induction of anesthesia with an intraperitoneal injection of ketamine (50 mg/kg body wt, Ketanest-S Parke-Davis/Pfizer, New York, NY, USA) and xylazine (50 mg/kg body wt, Rompun, Bayer AG, Leverkusen, Germany), pups were exsanguinated by transection of the abdominal blood vessels. The thoracic cavity was opened and the lungs were removed, snap-frozen in liquid nitrogen, and stored at -80°C until use for real-time RT-PCR or microarray analysis. For histology studies, the trachea was cannulated (Bioflow 0.6 mm iv catheter, Vygon, Veenendaal, Netherlands) and the lungs were perfusion-fixed in situ with buffered formaldehyde (3.8% paraformaldehyde in phosphate-buffered saline, pH 7.4) at 25 cm H_2O pressure for 3 min. Lungs were removed, fixed additionally in buffered formaldehyde for 24 h at 4°C , and embedded in paraffin after dehydration in a graded alcohol series and xylene. For studies of fibrin deposition, pups were injected with heparin (100 units, Leo Pharma, Breda, Netherlands) via the tail vein under Ketamine/Xylazine anesthesia. After 3 to 4 min, pups were exsanguinated by transection of the abdominal vessels; their lungs were removed, rinsed briefly in 0.9% NaCl, frozen immediately in liquid nitrogen, and stored at -80°C until use.

Lung Histology. Paraffin sections (4 μm) cut from the left upper lobe were mounted onto SuperFrost plus coated slides (Menzel-Gläzer, Germany). After deparaffinization, sections were stained with hematoxylin and eosin and a monoclonal antibody (ED1) against monocytes and macrophages (15). For immunohistochemistry, sections were incubated with 0.3% H_2O_2 in methanol to block endogenous peroxidase activity. After a graded alcohol series, sections were boiled in 0.01 M sodium citrate (pH 6.0) for 10 min. Sections were incubated overnight with ED1, stained with EnVision-HRP (Dako, Glostrup, Denmark), using NovaRed (Vector, Burlingame, CA, USA) as chromogenic substrate, and counterstained briefly with hematoxylin. For morphometry, an eye piece reticle with a coherent system of 21 lines and 42 points (Weibel type II ocular micrometer; Paes, Zoeterwoude, Netherlands) was used. Mean linear intercept (Lm), an indicator of mean alveolar diameter (36), was assessed in 10 nonoverlapping fields at a 200x magnification in one section for each animal. The density of ED1-positive monocytes and macrophages was determined by counting the number of cells per field and the number of points covering the alveolar tissue. Fields containing large blood vessels or bronchioli were excluded from the analysis. Results were expressed as cells per millimeter². Per experimental animal 22 fields in one section were studied at a 400x magnification. At least five different rat pups per experimental group were studied.

Fibrin detection assay. Pulmonary fibrin deposition was detected as described previously (54). Briefly, frozen lungs were homogenized with an Ultra-Turrax T8 tissue homogenizer (IKA-Werke, Staufen, Germany) for 1 min at full speed in a cold 10 mM sodium phosphate buffer (pH 7.5), containing 5 mM EDTA, 100 mM ϵ -aminocaproic acid, 10 U/ml aprotinin, 10 U/ml heparin, and 2 mM phenylmethanesulfonyl fluoride. The homogenate was incubated for 16 h on a top-over top rotor at 4°C. After centrifugation (10,000 rpm, 4°C, 10 min), the pellet was resuspended in extraction buffer (10 mM sodium phosphate buffer [pH 7.5], 5 mM EDTA, and 100 mM ϵ -aminocaproic acid) and centrifugated again (10,000 rpm, 4°C, 10 min). Pellets were suspended in 3 M urea, extracted for 2 h at 37°C, and centrifugated at 14,000 rpm for 15 min. After the supernatant was aspirated and discarded, the pellet was dissolved at 65°C in reducing sample buffer (10 mM Tris pH 7.5, 2% SDS, 5% glycerol, 5% β -mercaptoethanol, and 0.4 mg/ml bromophenol blue) for 90 min with vortexing every 15 min. Then, samples were subjected to SDS-PAGE (7.5%, 5% stacking) and blotted onto PVDF membrane (Immobilon-P, Millipore, Bedford, MA, USA). Fibrin β -chains were detected with a monoclonal antihuman fibrin antibody (59D8, Boston Research Services Company, Winchester, MA, USA) that specifically recognizes β -fibrin (26, 54), using chemiluminescence (ECL; Amersham, Arlington Heights, IL, USA) and Kodak X-OMAT Blue XB-1 films (Eastman Kodak, Rochester, NY, USA). Exposures were quantified with a Biorad GS-800 calibrated densitometer using the Quantity One, version 4 software package (Biorad, Veenendaal, Netherlands). Fibrin deposition was quantified in lungs of at least nine rats per experimental group. As a reference, fibrin standards were generated from rat fibrinogen (Sigma Chemical, Co., St. Louis, MO, USA). After rat fibrinogen was solubilized in two-thirds strength PBS (pH 7.4), human α thrombin (Sigma Chemical Co.) was added, vortexed, and incubated at 37°C for 10 min. After addition of 2x SDS sample buffer, the fibrin sample was vortexed, incubated at 65°C for 90 min, and aliquots were frozen at -80°C until use.

Generation of cRNA and chip hybridization. Total RNA was isolated from lung tissue homogenates using guanidium-phenol extraction (RNAzol; Campro Scientific, Veenendaal, Netherlands). Briefly, after tissue homogenization in RNAzol B, RNA was isolated using phenol-chloroform extraction and isopropanol precipitation. To avoid contamination with genomic DNA, the lowest part of the aqueous phase after phenol-chloroform extraction was not included in the total RNA sample. The RNA sample was dissolved in RNase-free water and quantified spectrophotometrically. The integrity of the RNA was studied by gel electrophoresis on a 1% agarose gel containing ethidium bromide. Samples showing degradation of ribosomal RNA by visual inspection under UV light (1 of 70 samples) were discarded. Equal amounts of total lung RNA of four rats were pooled and purified on RNeasy columns (Qiagen, Chatsworth, CA, USA); 20 μ g of total RNA was reverse transcribed (SuperScript Choice System, Life Technologies, Breda, Netherlands) using an oligo(dT)24 primer containing a T7 RNA polymerase promoter site added to the 3' end (Genset, La Jolla, CA, USA). The cDNA was used as a template for in vitro transcription with biotin-labeled nucleotides

(Enzo Diagnostics, Farmingdale, NY, USA). After fragmentation, 15 μg biotinylated cRNA was hybridized to Affymetrix GeneChip Rat Genome U34 arrays (Affymetrix, Santa Clara, CA, USA) for 16 h at 45°C at the Leiden Genome Technology Center. Four biotinylated hybridization controls were included in each hybridization reaction to verify consistent hybridization efficiency. Standard posthybridization washes and double-stain protocols were performed on a Genechip Fluidics Station 400 (Affymetrix). Arrays were scanned on a Hewlett Packard Gene Array scanner (Hewlett-Packard, Palo Alto, CA, USA).

Array data analysis. Scanned output files of arrays were analyzed by using Microarray Analysis Suite 5.0 (MAS5, Affymetrix). This software calculated signal intensities, detection calls (present or absent), and signal log ratios with confidence calls for increased or decreased gene expression ($p = 0.003$). The Wilcoxon's Signed Rank test was the statistical method employed to generate detection p values and change p values; signals and signal log ratios were calculated using the One-Step Tukey's Biweight Estimate. Genes were differentially expressed between oxygen-exposed and age-matched controls if both pair-wise comparisons yielded a consistent difference call and the mean ratio was at least 2.8. Genes that were not expressed at birth and in both oxygen-exposed and age-matched room air controls were excluded from the analysis. Gene expression was analyzed and clustered by generating self-organizing maps with the SOM analysis algorithm present in the Affymetrix Data Mining Tool software package (Affymetrix). Genes with a mean intensity of at least 50 and a maximum intensity of higher than 90 and that differed in intensity by at least 2-fold with a minimal difference between the highest and lowest value of 50 between experimental groups were included for clustering. Hereafter, genes with a difference of at least 2.8-fold between experimental groups were included for further analysis.

Real-time RT-PCR. Total RNA was isolated from a new set of rat pups, different from the samples used for the DNA chip experiment, and was quantified as described above. First-strand cDNA synthesis was performed with the SuperScript Choice System (Life Technologies) by mixing 2 μg total RNA with 1 μg oligo(dT)12-18 primer in a total volume of 10 μl . After heating the mixture at 70°C for 10 min, a solution containing 50 mM Tris-HCl (pH 8.3), 75 mM KCl, 3 mM MgCl_2 , 10 mM DTT, 0.5 mM dNTPs, 0.5 μl RNase inhibitor, and 200 U Superscript Reverse Transcriptase was added, resulting in a total volume of 20 μl . This mixture was incubated at 42°C for 1 h, with the total volume adjusted to 100 μl with RNase-free water, and stored at -80°C until further use. For real-time quantitative PCR, 5 μl of first-strand cDNA was used in a total volume of 25 μl that contained 12.5 μl of 2x SYBR Green PCR Master Mix (Applied Biosystems, Foster City, CA, USA) and 200 ng of each primer. Primers, designed with the Primer Express software package (Applied Biosystems), are listed in Table 1. PCR reactions, consisting of 95 °C for 10 min (1 cycle), 94 °C for 15 s, and 60 °C for 1 min (40 cycles), were performed on an ABI Prism 7700 Sequence Detection System (Applied Biosystems). Data were analyzed with the ABI Prism 7700 Sequence Detection System version 1.9 software and quantified using the

comparative threshold cycle (C_T) method with β -actin as a housekeeping gene reference (42). Data are expressed as mean \pm SEM relative to room air controls on day 3.

Gene Product	Forward Primer	Reverse Primer
Amphi-regulin	5'-TTTCGCTGGCGCTCTCA-3'	5'-TTCCAACCCAGCTGCATAATG-3'
CD14	5'-AAATTCCCAGACCCTCCAAGT-3'	5'-CCGCTGGTCGTCTCCATC-3'
c-Fos	5'-CAACGAGCCCTCCTCTGACT-3'	5'-TGCCTTCTCTGACTGCTCACA-3'
p21	5'-CATGTCCGATCCTGGTGATG-3'	5'-CGAACAGACGACGGCATACTT-3'
FGFR-4	5'-GTTGGCACGCAGCTCCTT-3'	5'-GCAGGACCTTGTCCAGAGCTT-3'
Flk-1	5'-CCACCCAGAAAATGTACCAAAC-3'	5'-AAAACGCGGGTCTCTGGTT-3'
Fra-1	5'-TTCTCCAGGACCCGTAAGTGA-3'	5'-TCAGAGAGGGTGTGGTCATGAG-3'
γ -FBG	5'-TGGGACAATGACAACGACAAG-3'	5'-TGTTTCATCCACCAGCCAGATC-3'
CINC-1	5'-GGGTGTCCCAAGTAATGGA-3'	5'-CAGAAGCCAGCGTTCACCA-3'
IL-6	5'-ATATGTTCTCAGGGAGATCTTGAA-3'	5'-TGCATCATCGCTGTTTCATACAA-3'
MCP-1	5'-TGGCAAGATGATCCCAATGA-3'	5'-AGCTTCTTTGGGACACCTGCT-3'
Met-1	5'-ATGTGCCAGGGCTGTGT-3'	5'-GCAGCACTGTTTCGTCACCTCA-3'
MMP-2	5'-CTGAGCTCCCGAAAAGATTG-3'	5'-CCTGCGAAGAACACAGCCTT-3'
MMP-9	5'-TCCGAGTCCAAGAAGATTTTC-3'	5'-GCACCGTCTGGCCTGTGTA-3'
MMP-12	5'-TCGTCTCTCTGCTGATGACATACA-3'	5'-GGATTTGTCAAGGATGGGTTTTT-3'
NGFI-B	5'-TGACGTGCAGCAATTTTATGACT-3'	5'-GGATCTTTCCGCCCACTTC-3'
PAI-1	5'-AGCTGGGCATGACTGACATCT-3'	5'-GCTGCTCTTGGTCGGAAAAGA-3'
PJunB	5'-GGCTTTGCGGACGTTTT-3'	5'-GGCGTCACGTGGTTCATCT-3'
SLPI	5'-TCTGATGCTTAACCCTCCAAT-3'	5'-GCCCTCACAACATTTGTATTTGC-3'
TF	5'-CCCAGAAAGCATACCAAGTG-3'	5'-TGCTCCACAATGATGAGTGTT-3'
TIMP-1	5'-AAGGGCTACCAGAGCGATCA-3'	5'-AGGTATTGCCAGGTGCACAAA-3'
TIMP-3	5'-GCCTTCTGCAACTCCGACA-3'	5'-CCCTTCCTTACCAGCTTCTT-3'
TM	5'-CTGGTGTGCTCATTGGGATCT-3'	5'-GACAAAGAAGCGCCAAAAGC-3'
TNF- α	5'-ACAAGGCTGCCCGACTAT-3'	5'-CTCCTGGTATGAAGTGGCAAATC-3'
Tpa	5'-TTCTTCTCTGACCGGCTGAAG-3'	5'-TGTTAAACAGATGCTGTGAGGTACAG-3'
Upa	5'-ACAGCCATCCAGGACCATACA-3'	5'-CCAAACGGAGCATCACCAA-3'
Upar	5'-TGCTGGGAAACCGGAGTTAC-3'	5'-GGAACCTTGGCACCAGGAA-3'
β -actin	5'-TTCAACACCCAGCCATGT-3'	5'-AGTGGTACGACCAGAGGCATACA-3'

Table 1. Sequences of oligonucleotides used as forward and reverse primers for real-time RT-PCR.

Statistics. Statistical analysis of the DNA array data is described in *Array data analysis*. Data of the RT-PCR, histopathological, and fibrin deposition studies are presented as mean \pm SEM. Statistical analysis was done using Student's *t*-test; $p \leq .05$ was considered statistically significant.

RESULTS

Survival, lung histology, morphometrical analysis, and fibrin deposition. At birth (day 1) body weight was 4.8 g (Figure 1A). In both oxygen-exposed and control pups body weight increased during the first week to approximately 10 g. From then on, controls grew slightly faster than oxygen-exposed pups. Initially, survival of both groups was similar (95%; Figure 1B). Lethal effects of hyperoxia were observed from day 8 onwards, resulting in a survival rate of 77% on day 10 and 15% on day 14. Therefore, we included only pups from birth until day 10 in our studies.

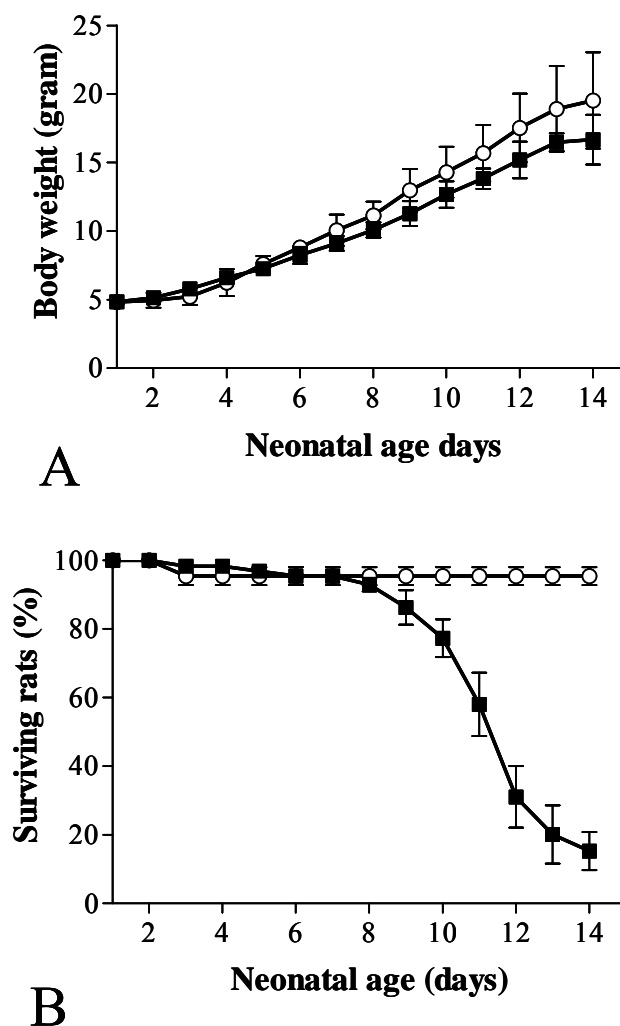


Figure 1. (A) Growth and (B) survival in oxygen-exposed rat pups (■) and room-air exposed littermates as controls (○) during the first 2 weeks after birth. Data are expressed as mean \pm SEM. Values were derived from four litters with 14 littermates on average and were corrected for mortality within 24 h after birth (approximately 10% in both oxygen-exposed and control pups).

Rats are born at the sacular stage of lung development (Figure 2A). From birth until day 3, terminal bronchioli branch into smooth-walled channels that ends in saccules. The septae of the newborn lungs are rather thick compared to later stages of development. Starting on day 6, alveoli are formed by secondary septation, resulting in a homogenous alveolar distribution by day 10 (Figure 2B). The Lm decreased by 32% from day 1 to day 10 (Figure 2D). Oxygen-induced changes in lung development were first observed on day 6. On days 6 and 10 (Figure 2C), sacculi continued to dominate amid a heterogenous distribution of alveoli due to local differences in secondary septation and septal thinning. Oxygen exposure resulted in a decreased number of irregularly enlarged air spaces and the Lm increased 15% and 39% on days 6 and 10, respectively, compared to age-matched controls (Figure 2D).

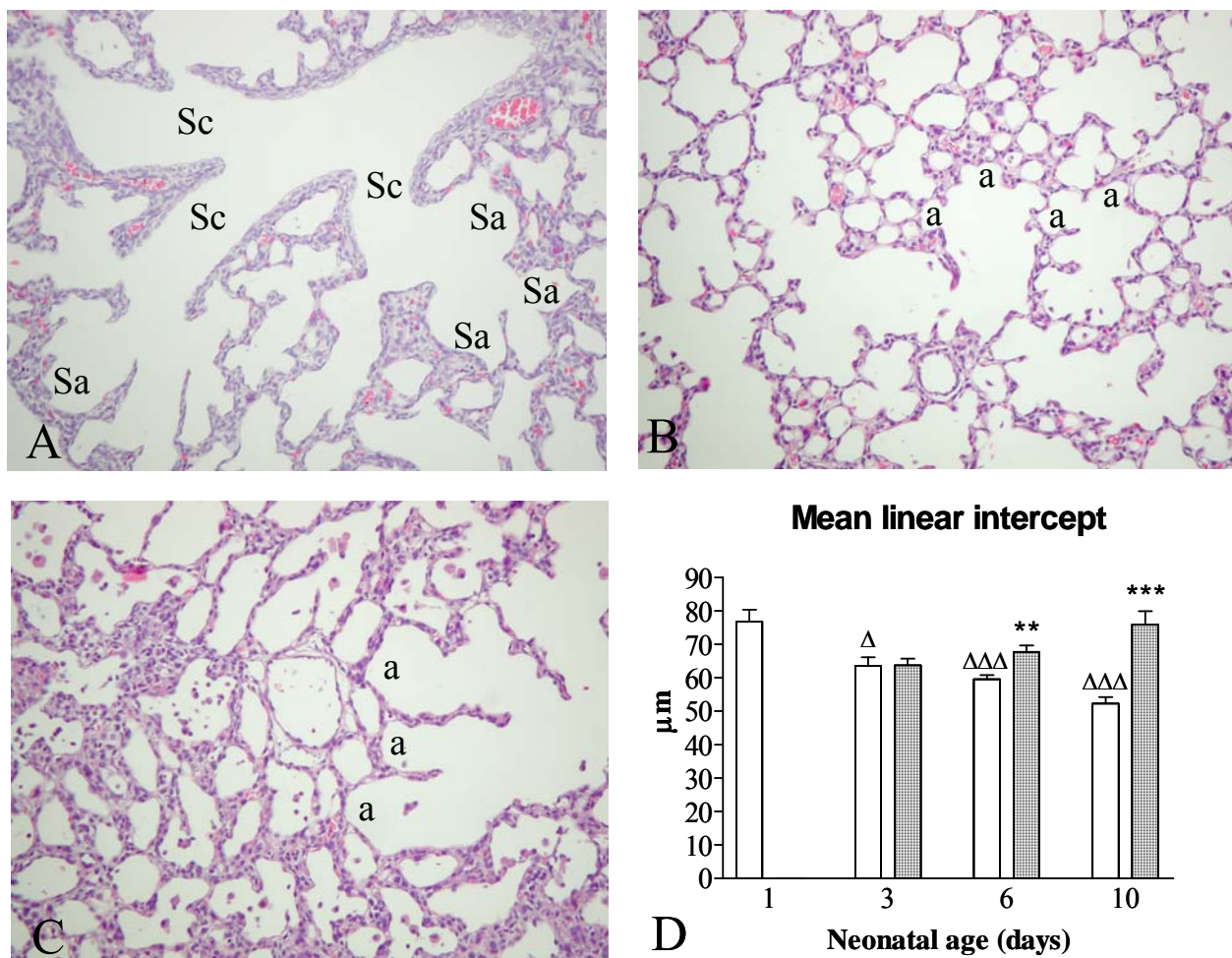


Figure 2. Development of the neonatal rat lung in formaldehyde-fixed and hematoxylin- and eosin-stained paraffin sections on (A) day 1 and (B) day 10 in control rat pups and (C) in an oxygen-exposed rat pup on day 10. All pictures were taken at a 200x magnification. (D) The mean linear intercept was determined in oxygen-exposed rat pups (gray bars) and room air-exposed littermates as controls (white bars). Data are expressed as mean \pm SEM in at least five different rat pups per group. a, alveolus; Sa, saccule; Sc, smooth walled channel. ** $p < 0.01$ and *** $p < 0.001$ vs. age-matched control. $\Delta p < 0.05$ and $\Delta\Delta\Delta p < 0.001$ vs. day 1.

On day 10, edema was observed in enlarged alveoli that were surrounded by septae with a marked increase in septal thickness (Figure 3A). By day 6, a massive inflammatory reaction was taking place, characterized by an overwhelming influx of neutrophilic granulocytes and macrophages in the alveolar septae and lumina (Figure 3A) and extravascular fibrin deposits in the air spaces (Figure 3B). Macrophages were detected with monoclonal ED1 (Figure 3C) and quantified by morphometry (Figure 3D). In control lungs, resident ED1-positive monocytes and macrophages were present at birth and remained constant at 190 cells/mm² alveolar tissue during the experimental period. However, in lungs of oxygen-exposed pups, the number of macrophages increased 2.7-fold and 6-fold on days 6 and 10, respectively.

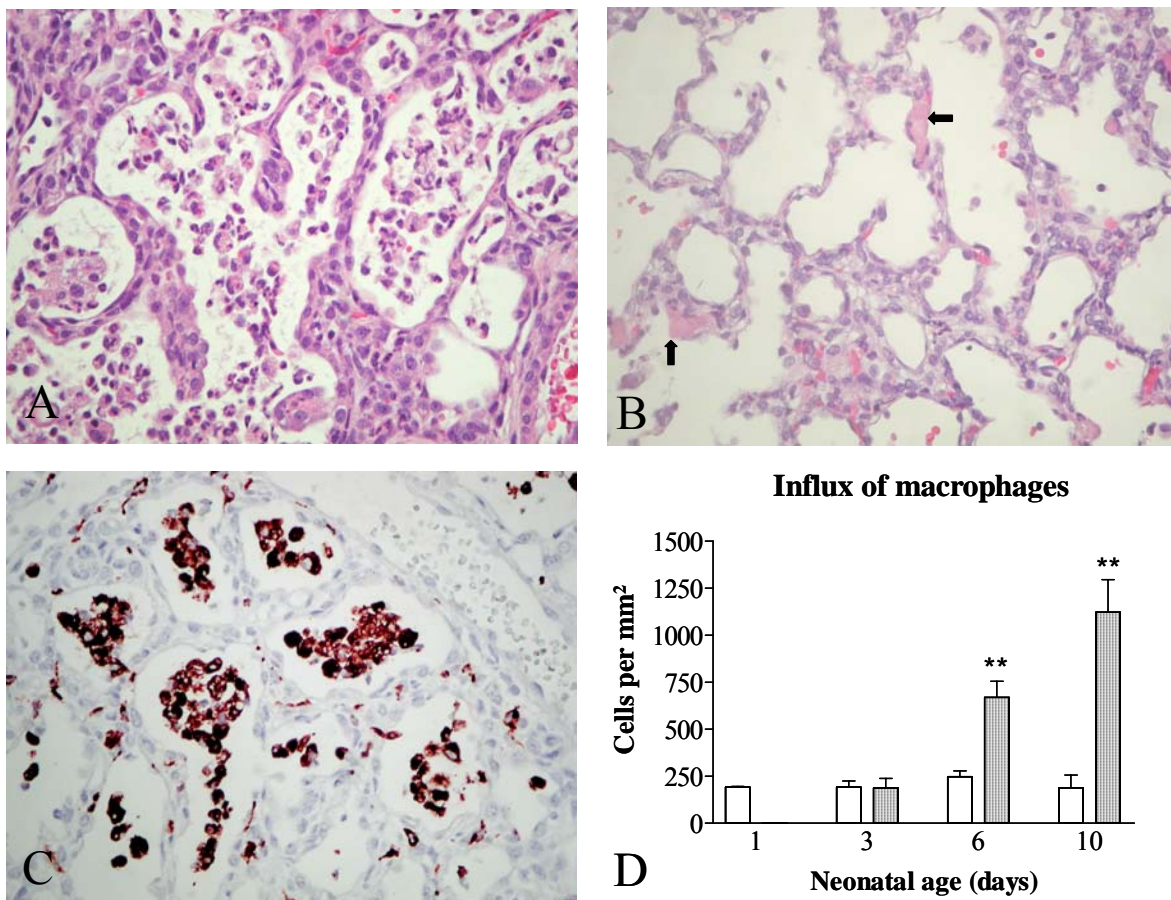


Figure 3. Formaldehyde-fixed and hematoxylin- and eosin-stained paraffin sections of neonatal rat lung after oxygen exposure on (A) day 10 and (B) day 6. (C) ED1 staining on a formaldehyde-fixed paraffin section of a rat lung on day 10 after oxygen treatment. All pictures were taken at a 400x magnification. (D) Quantification of ED1-positive monocytes and macrophages on paraffin sections in oxygen-exposed rat pups (gray bars) and room air-exposed littermates (white bars) as controls. Note the increase in septal thickness and the presence of large numbers of leukocytes, including neutrophilic granulocytes and macrophages in the enlarged alveolar lumen (A and D) and the presence of extravascular fibrin deposits on day 6 after oxygen-exposure (arrows in B). Data are expressed as mean \pm SEM in at least five different rat pups per group. ** $p < 0.01$ vs. age-matched control.

Differences in gene expression patterns by DNA array analysis. Gene expression of 8,799 cDNAs was investigated, of which 5,371 were present in at least one experimental group. Expression was studied in five experimental groups: birth (day 1), day 3 RA, day 3 O₂, day 10 RA, and day 10 O₂. The SOM Clustering Algorithm was used to generate 8 clusters (A-H) of genes that share a high degree of similarity in expression over time and oxygen exposure (Figure 4 and Appendix 1). Differentially expressed genes related to the birth process were observed in clusters A, D, E, and F (Table 2). Genes upregulated at birth were observed in clusters D (12 genes), E (16 genes), and F (10 genes). In cluster D, genes were found that were both upregulated on day 1 and after oxygen exposure on day 10. Cluster D contained 2 components of AP-1 (c-Fos and JunB), antioxidants metallothionein-1 and -2, immediate early genes (NGFI-A, -B, and TIS), and protein tyrosine phosphatase. Cluster E contained genes related to lipids (plasmalogen and phospholipase A2) and collagen α 1-II. Cluster F contained genes that were related to (cardiac) muscle including myosin heavy chains (Myh3, -7, and -8), myosin light chains (MLC1f and -2), troponins (troponin-C and -I), muscle C protein, and phosphoserine aminotransferase. Genes expressed at low levels at birth were observed in cluster A (four genes) and included the muscle proteins smooth muscle actin and transgelin, the extracellular matrix component tenascin-C, and 12-lipoxygenase.

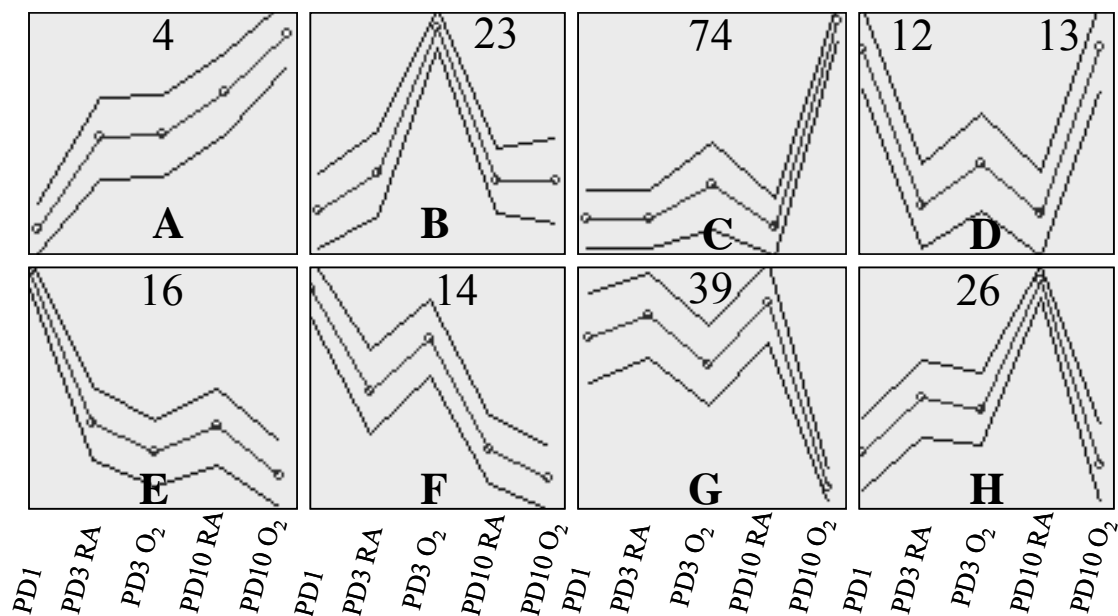


Figure 4. Cluster analysis by the generation of self-organizing maps (SOMs) with the SOM analysis algorithm of the entire expression data set. Genes with a mean intensity of at least 50 and a maximum intensity of higher than 90 and that differed in intensity by at least 2-fold with a minimal difference between the highest and lowest value of 50 between experimental groups were included in the SOM analysis. Thereafter, genes with a difference of at least 2.8-fold between experimental groups were included for further analysis. In each panel, average signal intensity is represented by the middle line connecting the experimental groups (\circ). The upper and lower lines show the standard deviation. The experimental groups include postnatal day 1 (PD1), day 3 RA (PD3 RA), day 3 O₂ (PD3 O₂),

day 10 RA (PD10 RA), and day 10 O₂ (PD10 O₂). Numbers in the top of each panel indicate the number of genes per cluster, except for cluster D. The number in the left upper corner represents the number of genes significantly upregulated at birth relative to PD3 RA, whereas the number in the right upper corner represents the number of genes significantly upregulated after hyperoxia at day 10 relative to PD 10 RA. Differentially expressed genes per cluster are listed in Appendix 1.

Gene	Cluster
Muscle-specific genes	
<i>Upregulated genes</i>	
[X15939] Myosin heavy chain 7 (4.8)	F
[M12098] Myosin heavy chain 3 (4.2)	F
[AI639532] Troponin C (3.5)	F
[K02423] Myosin light chain 1f (3.2)	F
[K02111] Myosin heavy chain 8 (3.1)	F
[X90475] Muscle C protein (3.1)	F
[X00975] Myosin light chain 2 (2.8)	F
[M73701] Troponin I (2.9)	F
<i>Downregulated genes</i>	
[M22323] Smooth muscle actin (-3.1)	A
[M83107] Transgelin (-2.8)	A
Antioxidants	
<i>Upregulated gene</i>	
[AI176456] Metallothionein 2 (3.3)	D
<i>Downregulated gene</i>	
[U09401] Tenascin-C (-5.0)	A
Signal transduction, transcription factors, and inflammation	
<i>Upregulated genes</i>	
[X06769] c-Fos (10.1)	D
[X51529] Phospholipase A2 (5.7)	E
[AF023087] NGFI-A (5.7)	D
[U17254] NGFI-B (3.4)	D
[X54686] JunB (3.3)	D
[AA900476] Cbp/p300 interacting transactivator 2; CITED2 (3.3)	E
[X63369] TIS (3.3)	E
Extracellular matrix	
<i>Upregulated gene</i>	
[AJ224879] Collagen α 1-II (4.8)	E

Table 2. Functional Groups of Selected Genes Substantially Up- or Downregulated in Lungs at Birth. Accession numbers are given between brackets and numbers in parentheses are average-fold changes relative to controls on postnatal day 3. Clusters are shown in Figure 4.

Differentially expressed genes in oxygen-exposed rats and their age-matched controls were observed in the clusters *B*, *C*, *D*, *G*, and *H* (Table 3). Genes upregulated in oxygen-exposed rats on day 10 were found in clusters *C* (74 genes) and *D* (13 genes). Genes downregulated in oxygen-exposed

rats on day 10 were found in clusters *G* (39 genes) and *H* (26 genes). Genes present in Clusters *C* and *D* showed a dramatic upregulation on day 10 in oxygen-exposed rat pups. Cluster *D* (13 genes) consisted of genes with two components of AP-1 (cFos and JunB), antioxidant genes (metallothionein-1, -2, and xanthine dehydrogenase), genes related to water transport and edema (aquaporin-3 and γ -atrial natriuretic peptide), and calgranulin A. Cluster *C* consisted of the largest number of genes (74), which were involved in inflammation, coagulation, fibrinolysis, DNA repair, oxygen detoxification, signal transduction, cell cycle, cell-cell interaction, and extracellular matrix turnover. The overwhelming inflammatory response and extravascular fibrin deposition observed with morphometrical analysis was confirmed by an increased expression of genes that encode cytokines (IL-6 and IL-1 β), chemokines and growth factors (CINC-1, MIP-2, MIC-1, MCP-1, amphiregulin, endothelin-1, and heparin-binding EGF-like growth factor), complement factors (complement proteins C1q β , C4, and C4-BP), immunoglobulins (Fc γ receptor, IgE-BP), procoagulant factors (TF and γ -FBG), and factors related to fibrinolysis (PAI-1, uPA, and uPAR). Hyperoxic lung injury was associated with the upregulation of genes that encode antioxidants, including metallothionein-1 and -2, hypoxanthine, heme-oxygenase and glutathion peroxidase, proteases (Osteopontin, MCP-7, MMP-12, protease-1), protease inhibitors (TIMP-1), genes that encode AP-1 (Fra-1, c-Fos, JunB), and the cell cycle-related genes cyclin G, the cyclin-dependent kinase inhibitor p21, and G0s2.

Gene	Cluster
Cytokines, chemokines, growth factors, and inflammation	
<i>Upregulated genes</i>	
[D11445] CINC-1 (42.2)	C
[M26744] IL-6 (40.8)	C
[U45965] MIP-2 (26.0)	C
[X55183] Amphiregulin (14.9)	C
[X17053] MCP-1 (8.0)	C
[AJ011969] MIC-1 (4.9)	C
[U78102] Egr-2 (4.3)	C
[Z22812] IL-1R type2 (3.7)	C
[AF087943] CD14 (3.2)	C
[K02814] MAPa1 (3.5)	C
[M64711] Endothelin 1 (3.5)	C
[L18948] MRP-14 (3.5)	C
[L05489] Heparin-binding EGF-like growth factor (3.3)	C
[M98820] IL-1 β (3.3)	C
Complement and immunoglobulins	
<i>Upregulated genes</i>	
[Z50051] C4BP α (27.9)	C
[X73371] Fc γ receptor (5.3)	C
[X71127] C1q β (4.0)	C
[U42719] C4 (3.2)	C
[J02962] IgE-BP (3.2)	C

Antioxidants and DNA repair	
<i>Upregulated genes</i>	
[AI176456] Metallothionein-2 (24.3)	D
[J02722] Heme oxygenase (6.1)	C
[AI102562] Metallothionein-1 (3.7)	D
[AI172247] Xantine dehydrogenase (3.7)	D
[AA800587] Glutathion peroxidase 2 (3.5)	C
[M76704] O-6-methylguanidine DNA methyltransferase (3.5)	C
Extracellular matrix, proteases, angiogenesis, and cytoskeleton	
<i>Upregulated genes</i>	
[M24067] Osteopontin (22.6)	C
[AI233219] Pineal specific protein (21.1)	C
[AA946503] Lipocalin-2 (17.5)	C
[U67910] Mast cell protease 7; MCP-7 (7.7)	C
[AJ005642] Brain serine protease; BSP-2 (5.9)	C
[X98517] MMP12 (4.0)	C
[AI169327] TIMP-1 (3.3)	C
[X81448] Keratin-18 (3.2)	C
[S69206] Protease-1 (3.1)	C
[D88250] Serine protease (3.0)	C
[S76054] Cytokeratin 8 (2.8)	C
<i>Downregulated genes</i>	
[U44845] Vitronectin (-4.9)	H
[R46974] Collagen α 1-III (-3.0)	H
Cell-cell interaction	
<i>Downregulated genes</i>	
[M76532] Connexin37 (-3.5)	G
[AI177621] ICAM-2 (-2.8)	H
[U77697] PECAM-1 (-2.8)	G
Coagulation and fibrinolysis	
<i>Upregulated genes</i>	
[U07619] Tissue factor (5.7)	C
[J00735] Fibrinogen γ (4.2)	C
[M24067] PAI-1 (16.0)	C
[X71898] uPAR-1 (6.5)	C
Receptors	
<i>Downregulated genes</i>	
[M91599] FGFR4 (-6.5)	G
[U93306] Flk-1 (-6.1)	G
[AI176031] TIE-1 (-3.5)	G
[U76206] VTR 15-20 (-3.3)	H
[U90610] CXCR-4 (-3.1)	G
[L04672] G protein coupled receptor (-3.0)	G
[U10995] Orphan receptor COUP-TFI (-2.8)	G
[X57764] ET-B endothelin receptor (-2.8)	G
Signal transduction, transcription factors, and cell cycle	
<i>Upregulated genes</i>	
[M19651] Fra-1 (16.0)	C

[L41275] p21 (12.1)	C
[Y00396] cmyc (4.3)	C
[X06769] c-Fos (3.5)	D
[U17254] NGFI-B (3.4)	D
[M65149] C/EBP δ (3.2)	C
[M18416] NGFI-A (3.2)	D
[X54686] pJunB (3.0)	D
[X70871] Cyclin G (3.0)	C
<i>Downregulated genes</i>	
[AA849036] Guanylate cyclase Ia3 (-7.5)	G
[AI011503] SOX-7 (-5.3)	G
[AA818381] c-kit proto-oncogene (-5.3)	G
[AA819900] Protocadherin α (-5.3)	H
[AA848639] cFos-induced growth factor (-4.3)	H
[AA893235] G0s2 (-3.7)	G
[AA997619] Cadherin V (-3.5)	G
[AI233225] Guanylate cyclase β 1(-3.2)	G
[U76032] cGMP-specific phosphodiesterase; PDE5 (-3.0)	G
[L09119] C kinase substrate calmodulin-binding protein RC3 (-3.0)	G
[AA875025] CRAB (-3.0)	H
[AA997870] Regulator of G-protein signaling 3; Rgs3 (-2.8)	G
[AA997477] Wnt2 (-2.8)	G
[AI103349] SOX-18 (-2.8)	G
Edema and water channels	
<i>Upregulated gene</i>	
[X01118] γ atrial natriuretic peptide; γ ANP (14.4)	D
[D17695] Aquaporin 3; AQP3 (4.3)	D

Table 3. Functional Groups of Selected Genes Substantially Up- or Downregulated in Lungs of Hyperoxia-Induced BPD on Postnatal Day 10. Accession numbers are given between brackets and numbers in parentheses are average-fold changes relative to controls on postnatal day 10. Clusters are shown in Figure 4.

Differences in gene expression patterns by real-time RT-PCR. To validate the findings obtained by cDNA chip analysis, expression of 27 genes with key roles in inflammation, coagulation, fibrinolysis, extracellular matrix turnover, cell cycle regulation, detoxification of oxidants, fibrosis, or alveolar enlargement was studied by real-time RT-PCR in lungs of oxygen-exposed and control pups on days 1, 3, 6, and 10. All genes studied with RT-PCR showed expression profiles similar to microarray data. These results strengthen and confirm the reliability of the microarray data.

Inflammation. At birth, elevated mRNA levels of the chemokines CINC-1 and MCP-1 and of CD14 were observed (Figure 5). Oxygen exposure resulted in a progressive increase in mRNA expression of the proinflammatory cytokines IL-6 and TNF- α , the chemokines CINC-1 and MCP-1, CD14, and the growth factor amphiregulin. The most marked changes in expression were seen in the oxygen-exposed pups on day 10, showing 292-fold, 15.5-fold, 10.9-fold, and 8.1-fold increases in mRNA expression compared to age-matched controls for IL-6, MCP-1, amphiregulin, and CINC-1, respectively.

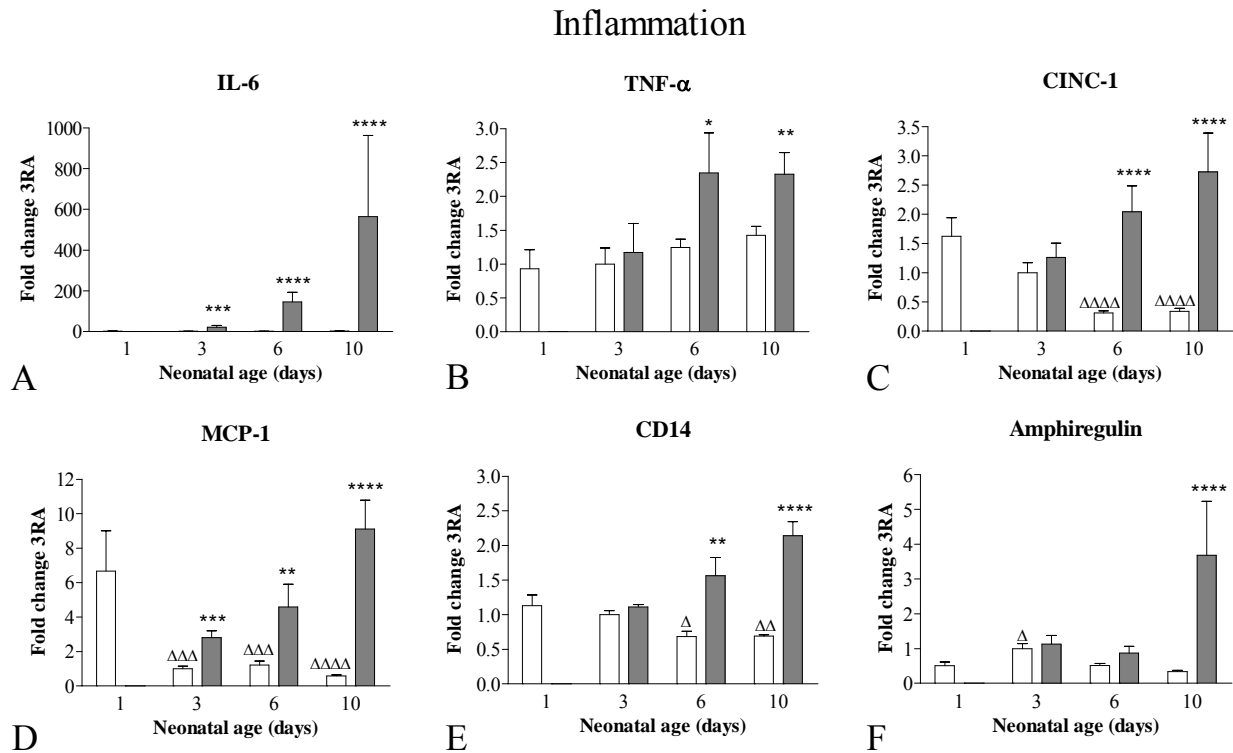


Figure 5. Relative mRNA expression, determined with RT-PCR, of genes related to inflammation (IL-6, TNF- α , CINC-1, MCP-1, CD14, and amphiregulin) in oxygen-exposed (gray bars) and control pups (white bars) on days 1, 3, 6, and 10. Data are expressed as mean \pm SEM of nine (day 1) or six (days 3, 6, and 10) rats. * p < 0.05; ** p < 0.01; *** p < 0.001; and **** p < 0.0001 vs. age-matched controls. Δp < 0.05; $\Delta\Delta p$ < 0.01; $\Delta\Delta\Delta p$ < 0.001; and $\Delta\Delta\Delta\Delta p$ < 0.0001 vs. day 1.

Coagulation and fibrinolysis. At birth, elevated levels of the procoagulants TF and γ -FBG (Figures 6A and 6B) and of the fibrinolytic factors uPA and uPAR (Figures 7B and 7C) were observed. uPAR expression decreased 8.3-fold from birth to day 10. Oxygen exposure resulted in a progressive upregulation of the procoagulant factors TF and γ -FBG, a downregulation of the anticoagulant thrombomodulin (TM), and an upregulation of the fibrinolytic factors uPA, uPAR, and PAI-1, but not tPA. On day 10, differential expression of the procoagulant TF and fibrinolytic inhibitor PAI-1 was 4.3-fold and 23.8-fold, respectively, higher in oxygen-exposed rats than in controls. The upregulation of TF and γ -FBG, downregulation of TM, and upregulation of PAI-1 may result in a procoagulant and antifibrinolytic environment (explained in Figure 8), which is indicative of disordered fibrin turnover (27, 28).

Coagulation

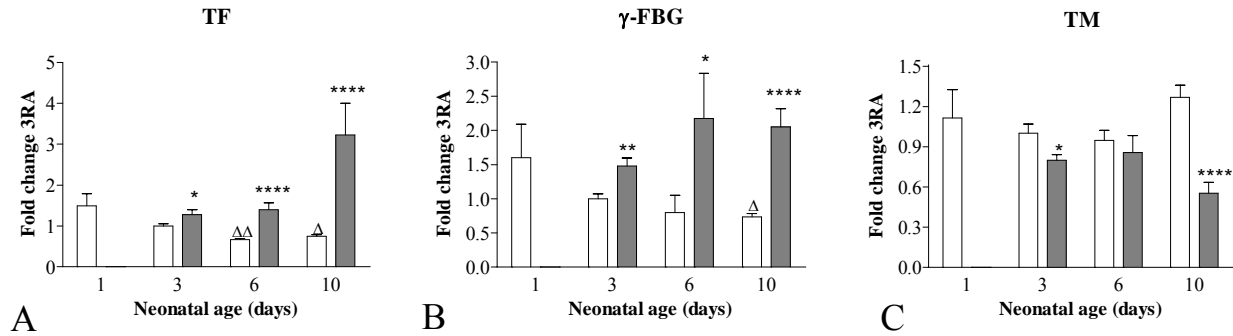


Figure 6. Relative mRNA expression, determined with RT-PCR, of genes related to coagulation (TF, γ -FBG, and TM) in oxygen-exposed (gray bars) and control pups (white bars) on days 1, 3, 6, and 10. Data are expressed as mean \pm SEM of nine (day 1) or six (days 3, 6, and 10) rats. * $p < 0.05$; ** $p < 0.01$; and **** $p < 0.0001$ vs. age-matched controls. $\Delta p < 0.05$ and $\Delta\Delta p < 0.01$ vs. day 1.

Fibrinolysis

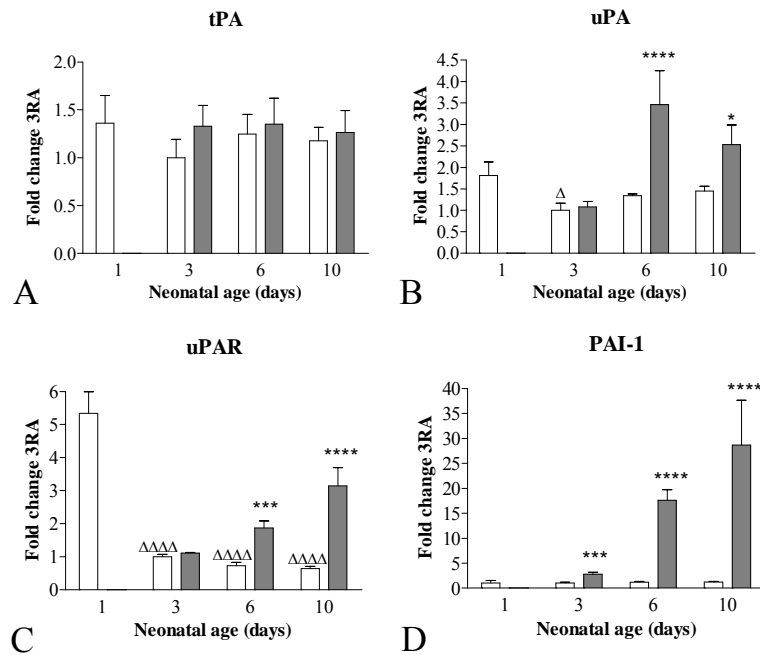


Figure 7. Relative mRNA expression, determined with RT-PCR, of genes related to fibrinolysis (tPA, uPA, uPAR, and PAI-1) in oxygen-exposed (gray bars) and control pups (white bars) on days 1, 3, 6, and 10. Data are expressed as mean \pm SEM of nine (day 1) or six (days 3, 6, and 10) rats. * $p < 0.05$; *** $p < 0.001$; and **** $p < 0.0001$ vs. age-matched controls. $\Delta p < 0.05$ and $\Delta\Delta\Delta\Delta p < 0.0001$ vs. day 1.

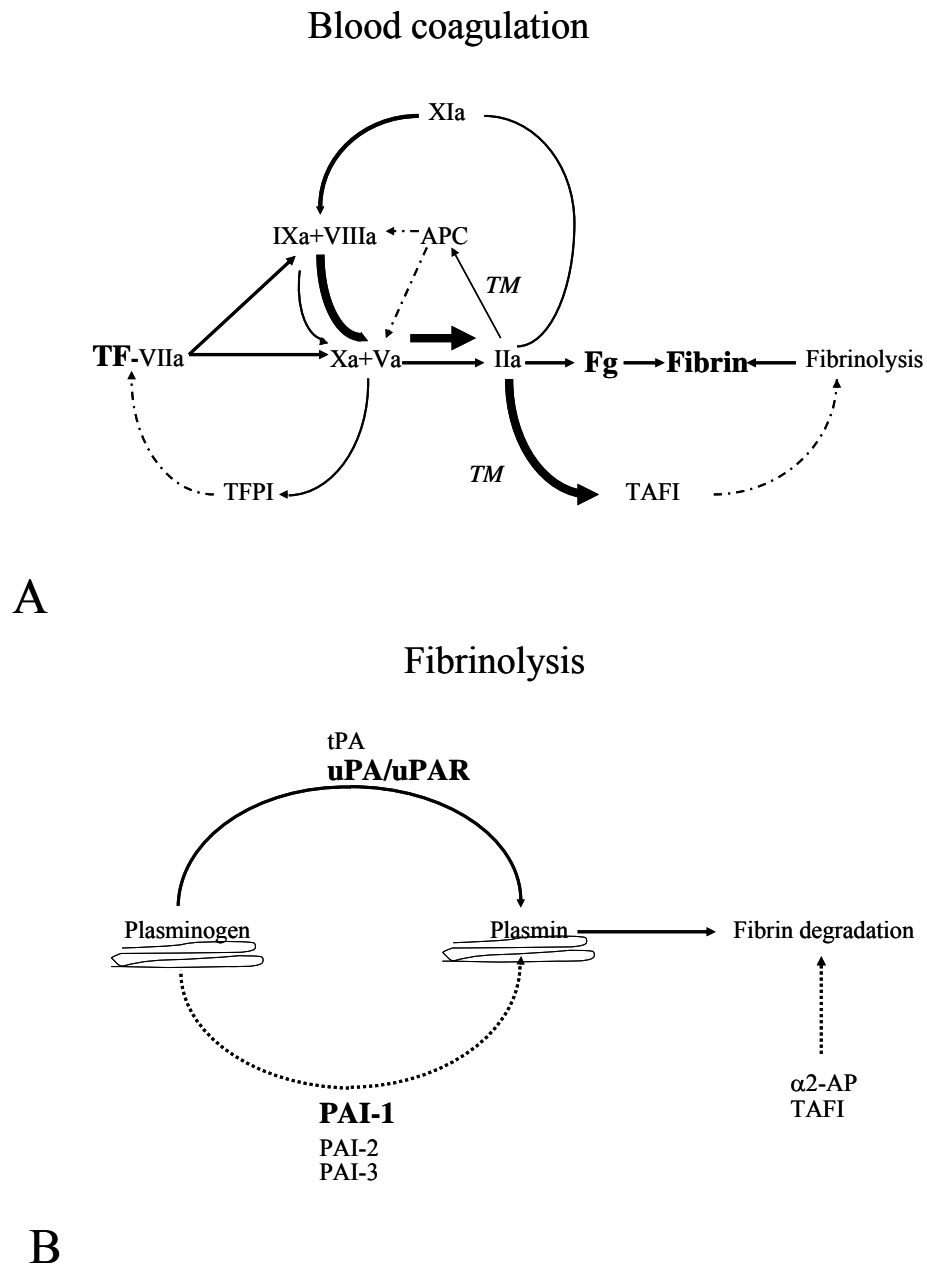


Figure 8. Schematic representation of the coagulation and fibrinolytic cascades. (A) Adapted from Bouma et al., *Thromb. Haemost.* **80**:24-27; 1998. Tissue damage results in the local expression of the physiological activator of the coagulation cascade tissue factor (TF). TF binds to factor VII/VIIa. (activated factor VII). This complex activates factors IX and X. Factor Xa activates prothrombin (factor II), resulting in thrombin (factor IIa) generation. Also, generation of factor Xa results in an inhibition of the extrinsic pathway by tissue factor pathway inhibitor (TFPI). At low concentration thrombin acts as an anticoagulant. After binding to its cofactor thrombomodulin (TM), thrombin activates protein C. Activated protein C (APC) inhibits the coagulation cascade by inactivation of factors VIIIa and Va, which act as cofactors of factors IXa and Xa, respectively. High concentrations of thrombin are procoagulant. It results in even higher thrombin concentrations via the factor XIa feedback loop. Proteolytic cleavage of fibrinogen (Fg) results in fibrin formation. Hyperoxia results in a local upregulation of TF and fibrinogen expression and a downregulation of TM expression, resulting in a procoagulant environment. High concentrations of thrombin are antifibrinolytic via the activation of thrombin-activatable fibrinolysis inhibitor (TAFI), bound to its cofactor TM. (B) Fibrinolysis is the process by which fibrin degradation takes place. Fibrin is degraded by plasmin after proteolytic cleavage of

plasminogen by plasminogen activators, i.e., tissue-type plasminogen activator (tPA) or urokinase-type plasminogen activator (uPA) bound to its receptor uPAR. Plasmin formation is regulated by plasminogen activator inhibitors (PAI-1, -2, and -3) of which PAI-1 is believed to be the most important PAI in fibrinolysis. Plasmin bound to the fibrin network is protected from inactivation by α 2-antiplasmin. Binding of plasmin to the fibrin network is prevented by TAFI, which removes the carboxyterminal lysines from the fibrin network that serve as binding sites for plasmin. Hyperoxia results in a moderate upregulation of the profibrinolytic factor uPA and its receptor uPAR, but not of tPA expression, and a tremendous upregulation of the inhibitor of fibrinolysis PAI-1. This will probably result in an antifibrinolytic environment. Hyperoxia results in a local procoagulant and antifibrinolytic environment, ultimately resulting in fibrin deposition in the developing neonatal lung. Solid lines indicate activation and dotted lines indicate inhibition. Factors in bold are upregulated and factors in *italic* are downregulated in our experiments.

Extravascular fibrin deposits were observed in septae and/or alveoli of oxygen-exposed lungs from day 6 onwards (Figure 3B). The deposition of fibrin was quantified by Western blotting and using an antibody against the 56 kDa fibrin β -chain. Since most antibodies recognize both fibrin and fibrinogen, the specificity for fibrin was investigated in fibrin- and in fibrinogen-containing samples. The 59D8 antibody recognizes fibrin but not fibrinogen (Figure 9A). Deposition of fibrin in lungs was observed at birth (Figures 9A and 9B), but was absent in control lungs thereafter. In oxygen-exposed pups, a progressive increase in fibrin deposition, of up to 80-fold on day 10 compared to controls, was observed.

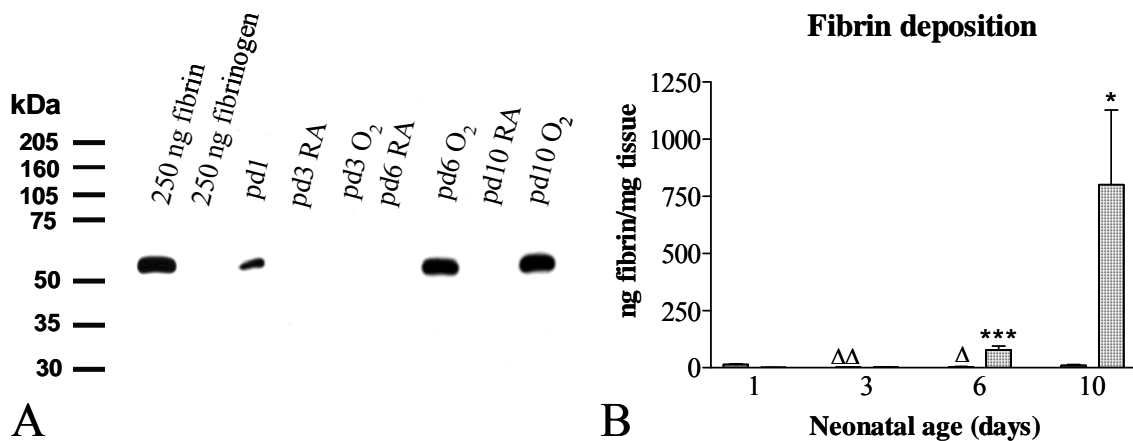


Figure 9. (A) Western blot analysis of fibrin deposition in lung homogenates of oxygen-exposed (O₂) and control (room air, RA) rat pups on days 1, 3, 6, and 10. The specificity of fibrin detection is demonstrated by the presence of the 56 kD thrombin-cleaved fibrin β -chain in a fibrin-containing sample (250 ng) but not in a fibrinogen-containing sample (250 ng). (B) Quantification of fibrin deposition in lung homogenates of control (white bars) and oxygen-exposed (gray bars) pups. Data are expressed as mean \pm SEM in at least nine different rat pups per group. * p < 0.05 and *** p < 0.001 vs. age-matched control. Δp < 0.05 and $\Delta\Delta p$ < 0.01 vs. day 1.

Extracellular matrix turnover, proteases, and protease-inhibitors. MMP-12 and SLPI showed a progressive increase in mRNA expression after birth (Figure 10). Hyperoxia-induced changes in mRNA expression were only observed for MMP-2, MMP-12, TIMP-1, and SLPI. The most marked increase in mRNA expression was observed for MMP-12 in oxygen-exposed pups on days 6 and 10, showing a 21.6-fold and 9.1-fold increase, respectively.

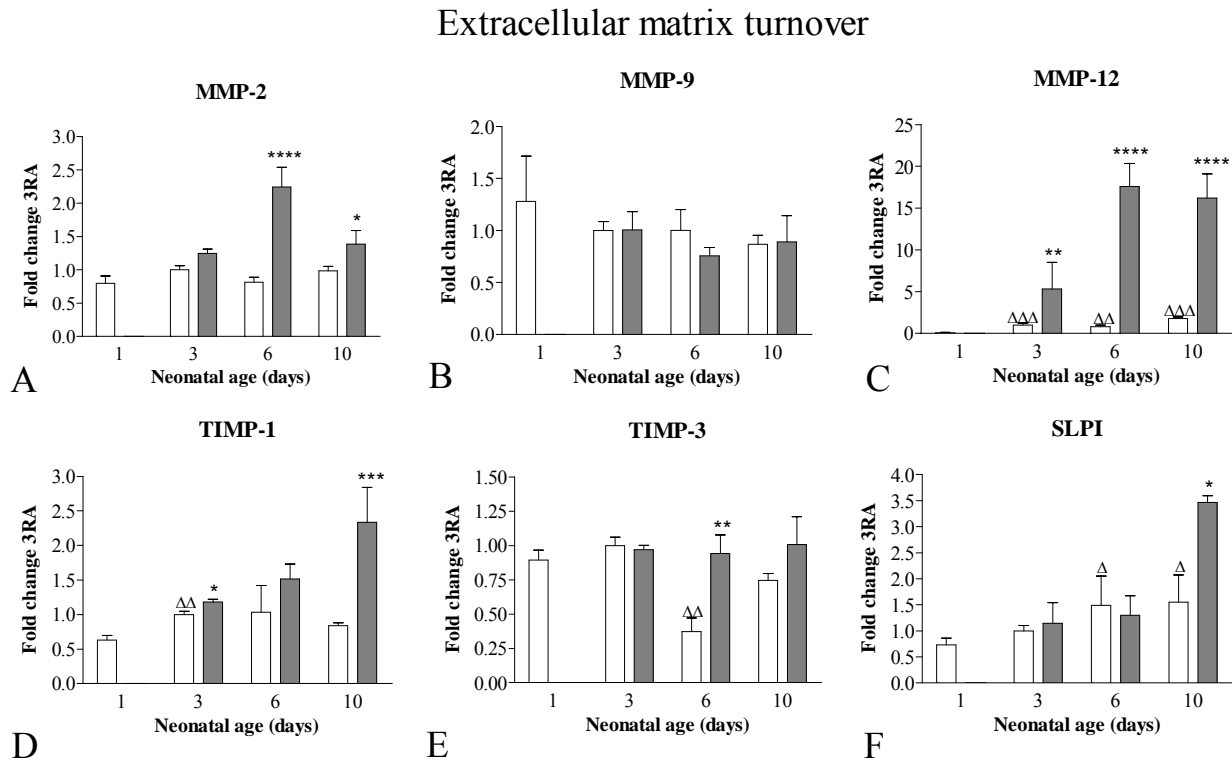


Figure 10. Relative mRNA expression, determined with RT-PCR, of genes related to extracellular matrix turnover (MMP-2, MMP-9, MMP-12, TIMP-1, TIMP-3, and SLPI) in oxygen-exposed (gray bars) and control pups (white bars) on days 1, 3, 6, and 10. Data are expressed as mean \pm SEM of nine (day 1) or six (days 3, 6, and 10) rats. * $p < 0.05$; ** $p < 0.01$; *** $p < 0.001$; and **** $p < 0.0001$ vs. age-matched controls. $\Delta p < 0.05$; $\Delta\Delta p < 0.01$; and $\Delta\Delta\Delta p < 0.001$ vs. day 1.

Signal transduction, cell cycle and anti-oxidants. At birth, elevated levels were observed of the AP-1 genes c-Fos and JunB (but not of Fra-1), the transcription factor NGFI-B, the cyclin-dependent kinase inhibitor p21, and the antioxidant Met-1 (Figure 11). In the controls, c-Fos and Met-1 mRNA expression decreased 51-fold and 13.3-fold, respectively, between birth and day 3. Hyperoxia-induced gene expression was observed for the AP-1 genes cFos and Fra-1, but not for JunB, and for NGFI-B, p21, and Met-1 (Figure 11).

Signal transduction, cell-cycle and anti-oxidants

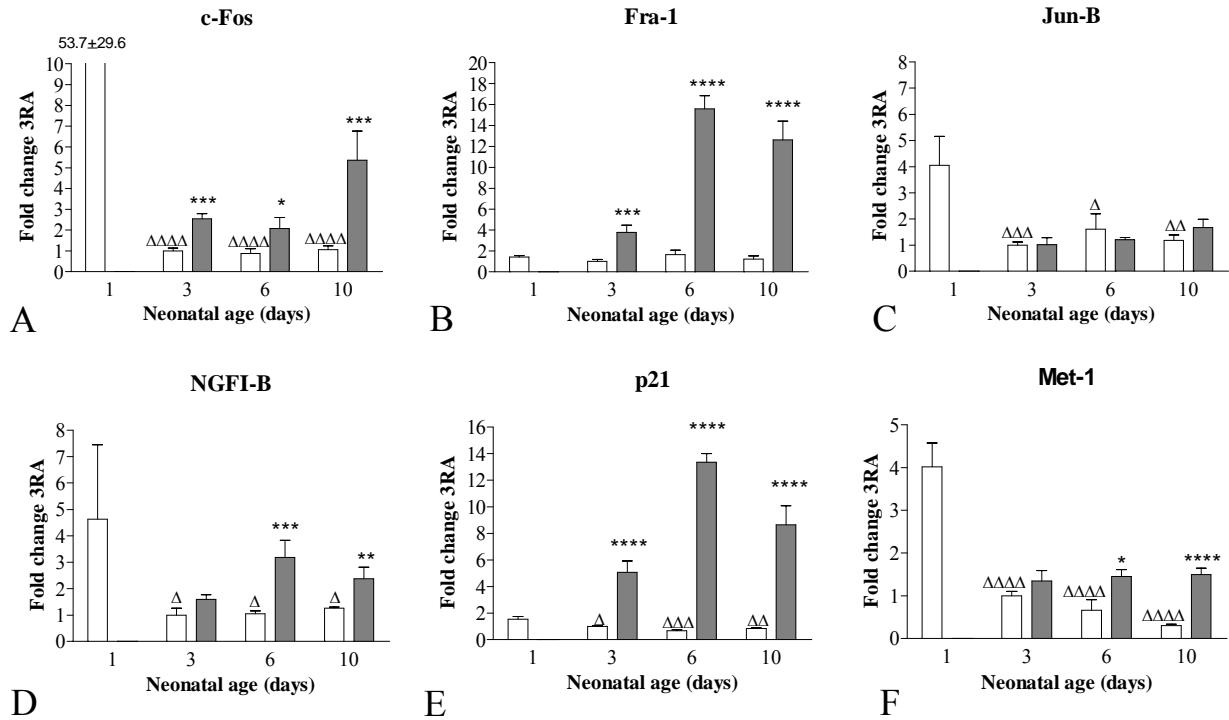


Figure 11. Relative mRNA expression, determined with RT-PCR, of genes related to signal transduction and cell cycle (AP-1: cFos, Fra-1, and Jun-B; NGFI-B; and p21) and of the antioxidant Met-1 in oxygen-exposed (gray bars) and control pups (white bars) on days 1, 3, 6, and 10. Data are expressed as mean \pm SEM of nine (day 1) or six (days 3, 6, and 10) rats. * $p < 0.05$; ** $p < 0.01$; *** $p < 0.001$; and **** $p < 0.0001$ vs. age-matched controls. $\Delta p < 0.05$; $\Delta\Delta p < 0.01$; $\Delta\Delta\Delta p < 0.001$; and $\Delta\Delta\Delta\Delta p < 0.0001$ vs. day 1.

Alveolar enlargement. In the first two weeks after birth, expression of membrane receptors related to alveolar enlargement showed either a gradual increase (FGFR-4) or a minor decrease (Flk-1, Figure 12). Both receptors were downregulated after hyperoxia. FGFR-4 expression was progressively downregulated, whereas Flk-1 mRNA expression was only downregulated on day 10.

Secondary septation and alveolar enlargement

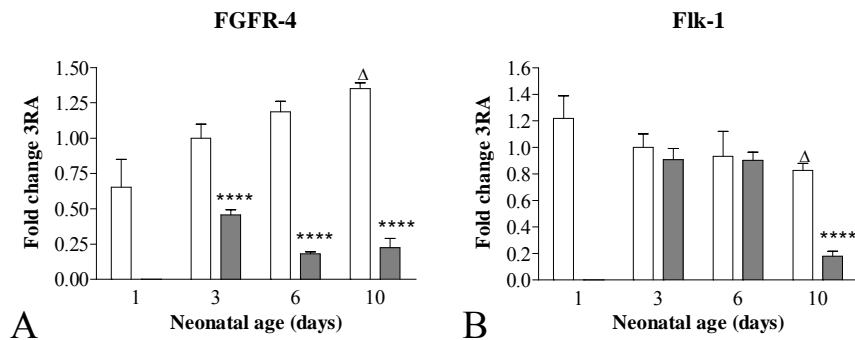


Figure 12. Relative mRNA expression, determined with RT-PCR, of genes related to fibrosis (FGFR-4) and emphysema (Flk-1) in oxygen-exposed (gray bars) and control pups (white bars) on days 1, 3, 6, and 10. Data are expressed as mean \pm SEM of nine (day 1) or six (days 3, 6, and 10) rats. **** $p < 0.0001$ vs. age-matched control. $\Delta p < 0.05$ vs. day 1.

DISCUSSION

In this study, we focused on differential gene expression in neonatal rat lungs exposed to *prolonged* hyperoxia with clear pathological changes during the *saccular* stage of development, an experimental setting that closely resembles the developmental stage of very premature infants receiving neonatal intensive care. Rats were born at the saccular stage of lung development and alveolarization by secondary septation took place during the first two weeks of life. Prolonged exposure of premature rat pups to 100% oxygen during this developmental process resulted in chronic lung injury, demonstrating the importance of oxidative stress in the development of BPD. The strength of this rat model is the accelerated development of BPD and a sequence of events similar to that in human premature infants (9). An inherent limitation of this model is that the most severely affected pups had already died on day 10 of hyperoxia and, therefore, did not contribute to the analysis of hyperoxia-responsive genes and histopathology of experimental BPD. This drawback may be circumvented by a much longer exposure at lower oxygen concentrations.

Using cDNA microarray analysis, largely confirmed by real-time RT-PCR, we demonstrated that prolonged oxidative stress affects a complex orchestra of genes involved in inflammation, coagulation, fibrinolysis, extracellular matrix turnover, cell cycle, signal transduction, and alveolar enlargement and is in line with the pathological changes seen in immature lungs developing BPD. This study is unique as it combines differential gene expression analysis by DNA chip technology and RT-PCR with histology, immunohistochemistry, and morphometry in immature lungs exposed to oxidative stress throughout the transformation from the saccular to the mature alveolarized stage. The picture that emerges is one of severe

inflammatory response in the first week of exposure to hyperoxia, which persists into the second week and is accompanied by a disturbed, heterogenous alveolar development due to a decrease in secondary septation, an increase in septal thickness, fibrin deposition, and fibrosis. The inflammatory response is characterized by an influx of leukocytes and a significant upregulation of mRNAs that encode proinflammatory cytokines, chemokines, proteinases, immunoglobulins, and complement factors. Though comparable morphological changes have been observed in newborn rats and mice exposed to hyperoxia (9, 53), differential gene expression has only been reported during the *early stages* of hyperoxia-induced injury in adult murine lungs when lung development has already advanced towards the *alveolar* developmental stage (41).

Functional activity of genes takes place at the protein level. Therefore, conclusions regarding protein function drawn on the basis of mRNA expression patterns are limited to those genes that are predominantly regulated at a (pre)transcriptional level. Nevertheless, the differential mRNA expression patterns presented in this study are in keeping with the pathological changes observed in immature lungs developing BPD.

Hyperoxia results in the generation of cytotoxic reactive oxygen species (ROS), either directly or indirectly by activation of leukocytes and the induction of cell death during the inflammatory response. Many genes that are differentially expressed can be transcriptionally activated by ROS, either directly by the upregulation of the stress response genes heme oxygenase (HO) and TNF- α or indirectly by the activation of the redox-responsive transcription factors AP-1 and/or NF- κ B (6, 18, 33, 46). AP-1 and/or NF- κ B induce gene expression of antioxidant enzymes, cytokines, chemokines, and growth factors (CINC-1, IL-6, IL-1 β , TNF- α , MIP-1, MIP-2, and MCP-1), matrix metalloproteinases (MMPs), coagulation factors (TF), and cell cycle proteins (p21). Transcriptional activation of components of AP-1 was observed for the Fos family members Fra-1 and c-Fos but not for Fra-2. Transcriptional activation of the Jun family members cJun and JunD by hyperoxia was not observed. Although, JunB transcription showed a 3-fold increase on day 3, these data could not be reproduced by RT-PCR. Expression of family members of NF- κ B was not studied.

One of the major effects of hyperoxia on lung development was the reduction of secondary septation and enlargement of alveoli, leading to irregular enlarged airspaces (emphysema). This phenomenon was accompanied by a downregulation of FGFR-4 from day 3 onwards and of Flk-1 on day 10. This confirms the observation that lungs of FGFR-3(-/-)/FGFR-4(-/-) mice are normal at birth, but have a complete block in alveogenesis and do not form secondary septae, demonstrating their cooperative function to promote the formation of alveoli (55). The downregulation of Flk-1 expression on day 10 coincided with the presence of enlarged alveoli and confirmed the findings in a similar rat model (25). Flk-1 is important for the maintenance of alveolar structures since mice treated with a Flk-1 inhibitor develop emphysema due to alveolar septal cell apoptosis (32). In the controls, FGFR-4 increased gradually in the first 2 weeks after birth, whereas Flk-1 showed only a minor decrease on day 10, similar to the expression

profile in neonatal mouse lung (37).

Many genes upregulated after hyperoxia are linked to the inflammatory response and involved in the activation and migration of leukocytes *in vivo*, including uPA/uPAR (21, 22, 44) and chemokines. The influx of granulocytes is mediated by chemokines, such as IL-8, CINC-1, and MIP-2, via the activation of the CXCR-2 receptor. The importance of these chemokines in hyperoxia-induced lung injury has been demonstrated by antichemokine treatment, which reduced neutrophil influx into the lungs and preserved alveolar development in newborn rats exposed to hyperoxia (2, 13).

The presence of extravascular fibrin deposits in septae and alveoli after the initiation of the inflammatory response, as demonstrated in this study, is a characteristic finding in the pathology of BPD (11). The presence of fibrin deposits in the lung soon after birth is probably due to tissue injury during birth. Lung injury at birth was further confirmed by the expression of genes in cluster *D*, such as members of AP-1, immediate early genes, and the antioxidant metallothionein-1, and by a local upregulation of procoagulants TF and γ -FBG. Intra-alveolar and extra- and intravascular fibrin deposition has been observed in acute lung injury (4, 27, 28), but the magnitude of its presence in BPD has not been previously studied and quantified. Fibrin deposition can be explained by disordered fibrin turnover, as demonstrated by our data on differential expression of genes related to coagulation and fibrinolysis during the inflammatory response. The upregulation of the procoagulant tissue factor (TF), downregulation of the anticoagulant thrombomodulin (TM), and upregulation of the fibrinolytic inhibitor PAI-1 yield a procoagulant and antifibrinolytic environment, resulting in fibrin deposition. Although the mRNAs of the fibrinolytic factors tPA and uPA are elevated in oxygen-exposed premature rat lungs, fibrinolytic activity is probably reduced by the presence of PAI-1-PA complexes (4).

The significance of PAI-1 in hyperoxia-induced fibrin deposition has been demonstrated in PAI-1-deficient mice, which failed to develop intra-alveolar fibrin deposits, showed a less severe phenotype, and were more resistant towards hyperoxia-induced mortality (4). Also, blocking of the coagulation cascade attenuates acute lung injury induced by gram-negative sepsis in baboons (8), indicating that inhibition of coagulation may have therapeutic importance in the treatment of BPD. Proinflammatory cytokines, IL-6 in particular, have a procoagulant effect, probably by stimulating TF expression on macrophages. Fibrinogen was upregulated in oxygen-exposed lungs, which indicates that the increased presence of extravascular fibrin(ogen) inside the alveoli is not only the result of plasma protein extravasation, but also due to local fibrinogen synthesis, possibly by stimulated lung epithelial cells. The accumulation of fibrin may contribute to lung injury in several ways. Fibrin can function as a ligand for cell adhesion molecules, including leukocyte integrin Mac1 (1, 17), and can facilitate cell migration and activation of inflammatory cells and fibroblasts, probably via activation of NF- κ B and AP-1 (49). Fibrin may, therefore, be both proinflammatory and profibrotic. Fibrin binds and inactivates lung surfactant (47, 48), which directly hampers pulmonary gas exchange (20).

Tissue remodelling by proteases, especially MMPs, plays an important role in many biological and pathophysiological processes, including acute lung injury and BPD (5, 38). MMP expression is controlled by growth factors and cytokines such as IL-1 and TNF- α . After 10 days of hyperoxia, we found an upregulation of many proteases including MMP-2 (gelatinase A) and MMP-12 (macrophage elastase) but not of MMP-9 (gelatinase B). This confirms the upregulation of these MMPs at the mRNA and protein level in lung tissue and lavage fluids of various other animal models (39, 40, 43). Enzyme activity of MMPs and serine proteinases is regulated by tissue inhibitors of matrix metalloproteinases (TIMPs) and SLPI (19). We observed an upregulation of TIMP-1 and SLPI mRNA expression. Oxidative stress upregulates SLPI expression in human epithelial cells (56), but this is the first report demonstrating that SLPI expression is increased as a result of oxidative stress *in vivo*. The increased SLPI expression may serve to provide protection against proteinase-mediated lung injury and infection. Interestingly, low SLPI levels in tracheobronchial aspirates of ventilated premature infants are associated with progress towards BPD (50). Also, our finding may be relevant for understanding cigarette smoke-induced lung cancer in adults, in view of the newly recognized role of this proteinase inhibitor in carcinogenesis (14). The significance of MMPs and TIMPs in lung injury has been demonstrated in knockout models. Lung injury was less severe in MMP-3-, MMP-9-, and MMP-12-deficient mice (51, 52), whereas TIMP-3-deficient mice showed spontaneous air space enlargement (34). MMP-12 plays a significant role in the development of emphysema since MMP-12-deficient mice are protected from cigarette smoke-induced emphysema (24).

Various genes in clusters *C* and *D*, which were upregulated by hyperoxia, play a critical role in the fibrotic response to bleomycin in the lung (31). This group of genes includes osteopontin, PAI-1, TIMP-1, HO, and JunB. Their upregulation suggests a potential role for fibrosis in the pathophysiology of BPD. PAI-1 upregulation impairs fibrinolytic activity in the alveolar compartment (4) and, as a result, PAI-1-deficient mice have a less severe phenotype after exposure to hyperoxia or bleomycin and are more resistant to oxidative stress than wild types (4, 16), whereas lung fibrosis is more severe in transgenic mice overexpressing PAI-1 (16).

By its nature, the screening approach used in this study can only identify the sum of changes throughout the entire lung, which will be necessarily biased against localized changes in gene expression. For example, VEGF has been shown in numerous hyperoxia and BPD models to be down-regulated (12), but it does not appear as significantly altered in these experiments.

In summary, this study demonstrates that oxidative stress induces a complex orchestra of genes involved in inflammation, coagulation, fibrinolysis, extracellular matrix turnover, cell cycle, signal transduction, and alveolar enlargement and explains, at least partially, the pathological alterations in neonatal lungs developing BPD. This knowledge is not only important in the understanding of the pathophysiology of BPD, but can also serve as a basis for the development of new therapeutic strategies.

ACKNOWLEDGMENTS

We thank Eveline M. Mank, Dr. Judith M. Boer, and Dr. Johan T. den Dunnen of the Leiden Genome Technology Center for expert technical assistance with the cDNA chip experiments. We gratefully acknowledge Dr. Joost C.M. Meijers for supplying us with the antibody 59D8. This study was supported in part by a grant from the Gisela Thier fund.

REFERENCES

1. **Altieri DC, Agbanyo FR, Plescia J, Ginsberg MH, Edgington TS and Plow EF.** A unique recognition site mediates the interaction of fibrinogen with the leucocyte integrin Mac-1 (CD11b/CD18). *J Biol Chem* 265: 12119-12122, 1990.
2. **Auten RL, Richardson RM, White JR, Mason SN, Vozzel MA and Whorton MH.** Nonpeptide CXCR 2 antagonist prevents neutrophil accumulation in hyperoxia-exposed newborn rats. *J Pharmacol Exp Ther* 299: 90-95, 2001.
3. **Bancalari E and Gonzalez A.** Clinical course and lung function abnormalities during development of neonatal chronic lung disease. *In chronic lung disease in early infancy. Edited by: Bland RD, Coalson JJ. New York: Marcel Dekker, 2000.*
4. **Barazzone C, Belin D, Piguet PF, Vassalli JD and Sappino AP.** Plasminogen activator inhibitor-1 in acute hyperoxic mouse lung injury. *J Clin Invest* 98: 2666-2673, 1996.
5. **Birkedal-Hansen H.** Proteolytic remodelling of extracellular matrix. *Curr Opin Cell Biol* 7: 728-735, 1995.
6. **Blackwell TS and Christman JW.** The role of nuclear factor- κ B in cytokine gene regulation. *Am J Respir Cell Mol Biol* 17: 3-9, 1997.
7. **Bonikos DS, Bensch KG, Ludwin SK and Northway WH Jr.** Oxygen toxicity in the newborn. The effect of prolonged 100 per cent O₂ exposure on the lungs of newborn mice. *Lab Invest* 32: 619-635, 1975.
8. **Carraway MS, Welty-Wolf KE, Miller DL, Ortel TL, Idell S, Ghio AJ, Petersen LC and Piantadosi CA.** Blockade of tissue factor: treatment for organ injury in established sepsis. *Am J Respir Crit Care Med* 167: 1200-1209, 2003.
9. **Chen Y, Martinez MA and Frank L.** Prenatal dexamethasone administration to premature rats exposed to prolonged hyperoxia: a new rat model of pulmonary fibrosis (bronchopulmonary dysplasia). *J Pediatr* 130: 409-416, 1997.
10. **Coalson JJ.** Experimental models of bronchopulmonary dysplasia. *Biol Neonate* 71: 35-38, 1997.
11. **Coalson JJ, Kuehl TJ, Escobedo MB, Hilliard JL, Smith F, Meredith K, Null DM Jr, Walsh W, Johnson D and Robotham JL.** A baboon model of bronchopulmonary dysplasia II. Pathologic features. *Exp Mol Pathol* 37: 335-350, 1982.
12. **D'Angio CT and Maniscalco WM.** The role of vascular growth factors in hyperoxia-induced injury to the developing lung. *Front Biosci* 7: d1609-d1623, 2002.
13. **Deng H, Mason SN and Auten RL Jr.** Lung inflammation in hyperoxia can be prevented by antichemokine treatment in newborn rats. *Am J Respir Crit Care Med* 162: 2316-2323, 2000.
14. **Devoogdt N, Hassanzadeh Ghassabeh G, Zhang J, Brys L, De Baetselier P and Revets H.** Secretory leucocyte protease inhibitor promotes the tumorigenic and metastatic potential of cancer cells. *Proc Natl Acad Sci USA* 100: 5778-5782, 2003.
15. **Dijkstra CD, Dopp EA, Joling P and Kraal G.** The heterogeneity of mononuclear phagocytes in lymphoid organs: distinct macrophage subpopulations in the rat recognized by monoclonal antibodies ED1, ED2, and ED3. *Immunology* 54: 589-599, 1985.
16. **Eitzman DT, McCoy RD, Zheng X, Fay WP, Shen T, Ginsburg D and Simon RH.** Bleomycin-induced pulmonary fibrosis in transgenic mice that either lack or overexpress the murine plasminogen activator inhibitor-1 gene. *J Clin Invest* 97: 232-237, 1996.
17. **Fan ST and Edgington T.** Integrin regulation of leucocyte inflammatory functions: CD11b/CD18 enhancement of the tumor necrosis factor- α responses to monocytes. *J Immunol* 150: 2972-2980, 1993.
18. **Fan J, Ye RD and Malik AB.** Transcriptional mechanisms of acute lung injury. *Am J Physiol Lung Cell Mol Physiol* 281: L1037-L1050, 2001.
19. **Gipson TS, Bless NM, Shanley TP, Crouch LD, Bleavins MR, Younkin EM, Sarma V, Gibbs DF, Tefera W, McConnell PC, Mueller WT, Johnson KJ and Ward PA.** Regulatory effects of endogenous protease inhibitors in acute lung inflammatory injury.

- J Immunol* 162: 3653-3662, 1999.
20. **Gupta M, Hernandez-Juviel JM, Waring AJ, Bruni R and Walther FJ.** Comparison of functional efficacy of surfactant protein B analogues in lavaged rats. *Eur Respir J* 16: 1129-1133, 2000.
 21. **Gyetko MR, Dud S, Sonstein J, Polak T, Sud A and Curtis JL.** Antigen-driven lymphocyte recruitment to the lung is diminished in the absence of urokinase-type plasminogen activator (uPA) receptor, but is independent of uPA. *J Immunol* 167: 5539-5542, 2001.
 22. **Gyetko MR, Sud S, Kendall T, Fuller JA, Newstead MW and Standiford TJ.** Urokinase deficient mice have impaired neutrophil recruitment in response to pulmonary *Pseudomonas aeruginosa* infection. *J Immunol* 165: 1513-1519, 2000.
 23. **Han RN, Buch S, Tseu I, Young J, Christie NA, Frndova H, Lye SJ, Post M and Tanswell AK.** Changes in structure, mechanics, and insulin-like growth factor-related gene expression in the lungs of newborn rats exposed to air or 60% oxygen. *Pediatr Res* 39: 921-929, 1996.
 24. **Hautamaki RD, Kobayashi DK, Senior RM and Shapiro SD.** Requirement of macrophage elastase for cigarette smoke-induced emphysema in mice. *Science* 277: 2002-2004, 1997.
 25. **Hosford GE and Olson DM.** Effects of hyperoxia on VEGF, its receptors and HIF-2 α in the newborn rat lung. *Am J Physiol Lung Cell Mol Physiol* 285: L161-L169, 2003.
 26. **Hui KY, Haber E and Matsueda GR.** Monoclonal antibodies to a synthetic fibrin-like peptide bind to human fibrin but not fibrinogen. *Science* 222: 1129-1132, 1983.
 27. **Idell S, James KK, Levin EG, Schwartz BS, Manchanda N, Maunder RJ, Martin TR, McLarty J and Fair DS.** Local abnormalities in coagulation and fibrinolytic pathways predispose to alveolar fibrin deposition in the adult respiratory distress syndrome. *J Clin Invest* 84: 695-705, 1989.
 28. **Idell S, Koenig KB, Fair DS, Martin TR, McLarty J and Maunder RJ.** Serial abnormalities of fibrin turnover in evolving adult respiratory distress syndrome. *Am J Physiol* 261: L240-L248, 1991.
 29. **Jobe AJ.** The new BPD: an arrest of lung development. *Pediatr Res* 46: 641-643, 1999.
 30. **Jobe AH and Bancalari E.** Bronchopulmonary dysplasia. *Am J Respir Crit Care Med* 163: 1723-1729, 2001.
 31. **Kaminski N, Allard JD, Pittet JF, Zuo F, Griffiths MJD, Morris D, Huang X, Sheppard D and Heller RA.** Global analysis of gene expression in pulmonary fibrosis reveals distinct programs regulating lung inflammation and fibrosis. *Proc Natl Acad Sci USA* 97: 1778-1783, 2000.
 32. **Kashara Y, Tudor DM, Taraseviciene-Stewart L, Le Gras TD, Abman S, Hirth PK, Waltenberger J and Voelkel NF.** Inhibition of VEGF receptors causes lung cell apoptosis and emphysema. *J Clin Invest* 106: 1311-1319, 2000.
 33. **Lander HM.** An essential role for free radicals and derived species in signal transduction. *FASEB J* 11: 118-124, 1997.
 34. **Leco KJ, Waterhouse R, Sanchez OH, Growing KLM, Poole AR, Wakeman A, Mak TW and Khokha R.** Spontaneous air space enlargement in the lungs of mice lacking tissue inhibitor of metalloproteinases-3 (TIMP3). *J Clin Invest* 108: 817-829, 2001.
 35. **Lemons JA, Bauer CR, Oh W, Korones SB, Papile LA, Stoll BJ, Verter J, Temprosa M, Wright LL, Ehrenkranz RA, Fanaroff AA, Stark A, Carlo W, Tyson JE, Donovan EF, Shankaran S and Stevenson DK.** Very low birth weight outcomes of the National Institute of Child health and human development neonatal research network, January 1995 through December 1996. NICHD Neonatal Research Network. *Pediatrics* 107: E1, 2001.
 36. **Margraf LR, Tomashefski JF Jr, Bruce MC and Dahms BB.** Morphometric analysis of the lung in bronchopulmonary dysplasia. *Am Rev Respir Dis* 143: 391-400, 1991.
 37. **Mariani TJ, Reed JJ and Shapiro SD.** Expression profiling of the developing mouse lung. Insights into the establishment of the extracellular matrix. *Am J Respir Cell Mol Biol* 26: 541-548, 2002.

38. **Nagase H and Woessner JF Jr.** Matrix metalloproteinases. *J Biol Chem* 274: 21491-21494, 1999.
39. **Pardo A, Barrios R, Maldonado V, Melendez J, Perez J, Ruiz V, Segura-Valdez L, Sznajder JI and Selman M.** Gelatinases A and B are up-regulated in rat lungs by subacute hyperoxia. *Am J Pathol* 153: 833-844, 1998.
40. **Pardo A, Selman M, Ridge K, Barrios R and Sznajder JI.** Increased expression of gelatinases and collagenases in rat lungs exposed to 100% oxygen. *Am J Respir Crit Care Med* 154: 1067-1075, 1996.
41. **Perkowski S, Sun J, Singhal S, Santiago J, Leikauf GD and Albelda SM.** Gene expression profiling of the early pulmonary response to hyperoxia in mice. *Am J Respir Cell Mol Biol* 28: 682-696, 2003.
42. **Pfaffl MW.** A new mathematical model for relative quantification in real-time RT-PCR. *Nucleic Acids Res* 29: e45, 2001.
43. **Radomski A, Sawicki G, Olson DM and Radomski MW.** The role of nitric oxide and metalloproteinases in the pathogenesis of hyperoxia-induced lung injury in newborn rats. *Br J Pharmacol* 125: 1455-1462, 1998.
44. **Rijneveld AW, Levi M, Florquin S, Speelman P, Carmeliet P and van der Poll T.** Urokinase receptor is necessary for adequate host defense against pneumococcal pneumonia. *J Immunol* 168: 3507-3511, 2002.
45. **Roberts RJ, Weesner KM and Bucher JR.** Oxygen-induced alterations in lung vascular development in the newborn rat. *Pediatr Res* 17: 368-375, 1983.
46. **Roebuck KA, Carpenter LR, Lakshminarayanan V, Page SM, Moy JN and Thomas LL.** Stimulus-specific regulation of chemokine expression involves differential activation of the redox-responsive transcription factors AP-1 and NF-kappaB. *J Leukoc Biol* 65: 291-298, 1999.
47. **Seeger W, Grube C and Gunther A.** Proteolytic cleavage of fibrinogen: amplification of its surfactant inhibitory capacity. *Am J Respir Cell Mol Biol* 9: 239-247, 1993.
48. **Seeger W, Stohr G, Wolf HR and Neuhof H.** Alteration of surfactant function due to protein leakage: special interaction with fibrin monomer. *J Appl Phys* 58: 326-338, 1985.
49. **Sitrin RG, Pan PM, Srikanth S and Todd RF 3rd.** Fibrinogen activates NF-kappa B transcription factors in mononuclear phagocytes. *J Immunol* 161: 1462-1470, 1998.
50. **Sveger T, Ohlsson K, Polberger S, Noack G, Morse H and Laurin S.** Tracheobronchial aspirate fluid neutrophil lipocalin, elastase- and neutrophil prorease-4- α 1-antitrypsin complexes, protease inhibitors and free proteolytic activity in respiratory distress syndrome. *Acta Paediatr* 91: 934-937, 2002.
51. **Warner RL, Beltran L, Younkin EM, Lewis CS, Weiss SJ, Varani J and Johnson KJ.** Role of stromelysin 1 and gelatinase B in experimental acute lung injury. *Am J Respir Cell Mol Biol* 24: 537-544, 2001.
52. **Warner RL, Lewis CS, Beltran L, Younkin EM, Varani J and Johnson KJ.** The role of metalloelastase in immune complex-induced acute lung injury. *Am J Pathol* 158: 2139-2144, 2001.
53. **Warner BB, Stuart LA, Papes RA and Wispe JR.** Functional and pathological effects of prolonged hyperoxia in neonatal mice. *Am J Physiol* 275: L110-L117, 1998.
54. **Weiler-Guettler H, Christie PD, Beeler DL, Healy AM, Hancock WW, Rayburn H, Edelberg JM and Rosenberg RD.** A targeted point mutation in thrombomodulin generates viable mice with a prethrombotic state. *J Clin Invest* 101: 1983-1991, 1998.
55. **Weinstein M, Xu X, Ohyama K and Deng CX.** FGFR-3 and FGFR-4 function cooperatively to direct alveogenesis in the murine lung. *Development* 125: 3615-3623, 1998.
56. **Yoneda K, Peck K, Mann-Jong M, Chmiel K, Sher YP, Chen J, Yang PC, Chen Y and Wu R.** Development of high-density DNA microarray membrane for profiling smoke- and hydrogen peroxide-induced genes in a human bronchial epithelial cell line. *Am J Respir Crit Care Med* 164: S85-S89, 2001.

LIST OF ABBREVIATIONS

AP-1	activator protein-1
BPD	bronchopulmonary dysplasia
FGFR	fibroblast growth factor receptor
Flk-1	vascular endothelial growth factor (VEGF) receptor-2
Fra-1	fos-related antigen-1
CINC-1	chemokine-induced neutrophilic chemoattractant-1
HO	heme oxygenase
γ -FBG	γ -fibrinogen
IL	interleukin
Lm	mean linear intercept
MCP-1	monocyte chemoattractant protein-1
Met-1	metallothionein-1
MIP-2	macrophage inflammatory protein-2
MMP	matrix metalloproteinase
NF- κ B	nuclear factor- κ B
NGFI-B	nerve growth factor-induced gene-B
PAI-1	plasminogen activator inhibitor-1
RA	room air
ROS	reactive oxygen species
SLPI	secretory leukocyte proteinase inhibitor
TIMP	tissue inhibitor of matrix metalloproteinases
TF	tissue factor
TM	thrombomodulin
TNF- α	tumor necrosis factor- α
tPA	tissue-type plasminogen activator
uPA	urokinase-type plasminogen activator
uPAR	urokinase-type plasminogen activator receptor

APPENDIX 1

Differentially expressed genes after cluster analysis by the generation of self-organizing maps (SOMs) of the entire expression data set. Genes with a mean intensity of at least 50 and a maximum intensity of higher than 90, and that differed in intensity by at least 2-fold with a minimal difference between the highest and lowest value of 50 between experimental groups were included for cluster analysis. Thereafter, genes with a difference of at least 2.8-fold between experimental groups were included for further analysis. Accession numbers are given in brackets and numbers in parentheses are average-fold changes relative to controls. Clusters are depicted in Figure 4.

Cluster A

Genes downregulated at birth compared to controls (room air) on day 3 are as follows:

- [U09401] Tenascin C (-4.9)
- [L06040] 12-lipoxygenase (-4.7)
- [M22323] γ -enteric smooth muscle actin (-3.1)
- [M83107] Transgelin (-2.8)

Cluster B

Genes upregulated by hyperoxia compared to room air on day 3 are as follows:

- [AA945169] EST (91.8)
- [AA945321] EST (56.9)
- [AA860062] Albumin (49.5)
- [X16273] Serine proteinase inhibitor-like protein (45.7)
- [D10261] 59 kDa bone sialic acid-containing protein (26.7)
- [AA866237] EST (24.4)
- [AI010453] EST (22.5)
- [M86240] Fructose-1,6-biphosphatase (20.8)
- [X02361] α -fetoprotein (20.4)
- [X63446] Fetuin (19.4)
- [M35601] α -fibrinogen (9.6)
- [J02597] Apolipoprotein A1 (7.7)
- [AA945169] EST (7.3)
- [M62642] Hemopexin (6.0)
- [X15512] Apolipoprotein C1 (5.7)
- [X78848] Glutathione S-transferase Yc subunit (4.5)
- [AB008423] CYP2D2 (4.3)
- [X83231] Pre- α -inhibitor, heavy chain 3 (4.1)
- [M10934] Spp-24 precursor (4.0)
- [U83880] Glycerol-3-phosphate dehydrate dehydrogenase (3.1)
- [D38380] Transferin (3.1)
- [M10934] Retinol-binding protein (2.9)
- [U31866] Nclone 10 (2.8)

Cluster C

Genes upregulated by hyperoxia compared to room air on day 10 are as follows:

- [D11445] CINC-1 (42.2)
- [M26744] IL-6 (40.8)
- [Z50051] C4BP α (27.9)
- [U45965] MIP-2 (26.0)
- [M24067] Osteopontin (22.6)

[AI233219] Pineal specific protein (21.1)
[M57263] Glutamine γ glutamyltransferase (19.6)
[AA946503] Lipocalin-2 (17.5)
[M24067] PAI-1 (16.0)
[M19651] Fra-1 (16.0)
[X13309] WDMN1 (15.6)
[X55183] Amphiregulin (14.9)
[L41275] p21 (12.1)
[X17053] MCP-1 (8.0)
[L12025] Tumor-associated glycoprotein E4 (8.0)
[D15069] Adrenomedullin precursor (7.9)
[U67910] Mast cell protease 7; MCP-7 (7.7)
[X71898] uPAR-1 (6.5)
[AB005900] Endothelial receptor for oxidized low-density lipoprotein (6.5)
[X71898] uPAR-1 (6.5)
[J02722] Heme oxygenase (6.1)
[M81855] MDR (6.0)
[AJ005642] Brain serine protease; BSP-2 (5.9)
[U07619] Tissue factor (5.7)
[AA799804] DLC1; mouse (5.5)
[X73371] Fc γ receptor (5.3)
[AJ011969] MIC-1 (4.9)
[U78102] Egr-2 (4.3)
[J00735] Fibrinogen gamma (4.2)
[AJ011969] SBF (4.8)
[AB010999] Peptidylarginine deiminase IV (4.8)
[X96437] PRG1 (4.6)
[D30649] Phosphodiesterase 1 (4.4)
[U78102] Krox20 (4.3)
[K02814] MAP α 1 (4.3)
[Y00396] c-myc oncogene (4.3)
[J05495] Gal/GalNac-specific lectin (4.2)
[U87627] MCT3 (4.2)
[X98517] MMP12 (4.0)
[AA875126] EST (4.0)
[M63282] Leucine zipper protein (4.0)
[X71127] C1q β (4.0)
[U67914] Mast cell carboxypeptidase A (3.8)
[J03624] Galanin (3.7)
[M91466] α 2b-adenosine receptor (3.7)
[Z22812] IL-1R type2 (3.7)
[AF087943] CD14 (3.2)
[K02814] MAP α 1 (3.5)
[M64711] Endothelin 1 (3.5)
[M98049] Pancreatitis-associated protein (3.5)
[L18948] MRP-14 (3.5)
[AA800587] Glutathion peroxidase 2; mouse (3.5)
[M76704] O-6-methylguanidine DNA methyltransferase (3.5)

[AA800709] EST (3.5)
[U36992] Cytochrome P450 Cyp7b1 (3.3)
[AI169327] TIMP-1 (3.3)
[L05489] Heparin-binding EGF-like growth factor (3.3)
[M98820] IL-1 β (3.3)
[U42719] Complement factor C4 (3.2)
[U50736] Cardiac adriamycin responsive protein (3.2)
[AF036537] Homocysteine respondent protein 2 (3.2)
[J02962] IgE-BP (3.2)
[X81448] Keratin-18 (3.2)
[AA799773] EST (3.2)
[M65149] C/EBP δ (3.2)
[AA875126] EST (3.1)
[S69206] Protease-1 (3.1)
[D88250] Serine protease (3.0)
[X70871] Cyclin G (3.0)
[X73911] Amiloride binding protein (2.9)
[AA894004] Macrophage capping protein; mouse (2.9)
[X59737] Ubiquitous mtochondrial creatine kinase (2.8)
[D14441] NAP-22 (2.8)
[S76054] Cytokeratin 8 (2.8)

Cluster D

Genes upregulated by hyperoxia compared to room air on day 10 are as follows:

[AI176456] Metallothionein-2 (24.3)
[X01118] γ atrial natriuretic peptide; γ ANP (14.4)
[D26393] Hexokinase II (12.8)
[X07266] Gene 33 polypeptide (6.9)
[D17695] Aquaporin 3; AQP3 (4.3)
[AI102562] Metallothionein-1 (3.7)
[AI172247] Xantine dehydrogenase (3.7)
[X06769] c-Fos (3.5)
[U17254] NGFI-B (3.4)
[M18416] NGFI-A (3.2)
[X54686] pJunB (3.0)
[J04791] Ornithine decarboxylase (3.0)
[AA957003] Calgranulin A (2.8)

Cluster D

Genes upregulated at birth compared to controls (room air) on day 3 are as follows:

[X06769] c-Fos (10.1)
[S74351] Protein tyrosine phosphatase (6.8)

[U75397] Krox-24 (6.5)
[AF023087] NGFI-A (5.7)
[S81478] Oxidative stress-inducible protein tyrosine phosphatase (5.5)
[U02553] Protein tyrosine phosphatase (5.0)
[U17254] NGFI-B (3.6)
[AI176456] Metallothionein 2 (3.3)
[X54686] JunB (3.3)
[M11794] Metallothionein 1 and 2 (3.2)
[AA800613] EST (3.1)
[AI176662] EST (2.9)

Cluster E

Genes upregulated at birth compared to controls (room air) on day 3 are as follows:

[J00738] α 2 macroglobulin (22.9)
[Z49858] Plasmalipin (16.1)
[S53527] S-100 β subunit (15.7)
[X86003] Neuron-derived orphan receptor 2 (8.0)
[AI639088] EST (7.0)
[X51529] Phospholipase A2 (5.7)
[AI045794] EST (4.9)
[AJ224879] Collagen α 1-II (4.8)
[L19660] Gastric inhibitory peptide receptor (4.7)
[AA900476] Cbp/p300 interacting transactivator 2; CITED2 (3.3)
[X63369] TIS (3.3)
[AF036761] Stearoyl-CoA desaturase 2 (3.1)
[X62951] pBUS19 (3.0)
[D84336] ZOG (2.8)
[D83349] Short type PB-cadherin (2.8)
[L19998] Minoxidil sulfotransferase (2.8)

Cluster F

Genes upregulated at birth compared to room air on day 3 are as follows:

[X15939] Myosin heavy chain 7 (4.8)
[M12098] Myosin heavy chain 3 (4.2)
[AI639532] Troponin C (3.5)
[K02423] Myosin light chain 1f (3.2)
[K02111] Myosin heavy chain 8 (3.1)
[X90475] Muscle C protein (3.1)
[X00975] Myosin light chain 2 (2.8)
[M73701] Troponin I (2.9)
[AI230228] Phosphoserine aminotransferase (2.8)
[X64827] Cytochrome c oxidase; subunit VIII-h (2.8)

Cluster F

Genes upregulated by hyperoxia compared to room air on day 3 are as follows:

[M19647] Kallikrein (6.3)
[M73701] Troponin I (3.6)
[M12098] Sarcomeric myosin heavy chain (3.5)
[K02423] Myosin light chain 1-f (3.3)
[AI639532] Troponin C (3.3)
[M99223] Calcium transporting ATPase (3.0)
[AI136540] EST (2.9)
[X00975] Myosin light chain 2 (2.8)
[X64827] Cytochrome c oxidase; subunit VIII-h (2.6)

Cluster G

Genes downregulated by hyperoxia compared to room air on day 10 are as follows:

[H31363] Pex14 (-17.0)
[AA849036] Guanylate cyclase Ia3 (-7.5)
[S35751] 3 α hydroxysteroid dehydrogenase (-6.8)
[M91599] FGFR4 (-6.5)
[U93306] Flk-1 (-6.1)
[AA945737] EST (-5.4)
[AI011503] SOX7 (-5.3)
[AA818381] c-kit proto-oncogene (-5.3)
[U03416] D2Sut1e (-5.2)
[Z29649] Periaxin (-4.5)
[U30832] B/K protein (-4.3)
[AA945054] Cytochrome b5 (-4.1)
[M30691] Ly6-C antigen (-4.0)
[AA893235] G0s2 (-3.7)
[AI227608] EST (-3.7)
[AI169372] EST (-3.6)
[AA686870] NADH-ubiquinone oxidoreductase, MLRQ subunit (-3.6)
[D38101] L-type voltage-dependent calcium channel α 1 subunit (-3.6)
[L36664] Kininase II (-3.6)
[Z17223] Gax protein (-3.5)
[M76532] Connexin37 (-3.5)
[AA997619] Cadherin V (-3.5)
[AI176031] TIE-1 (-3.5)
[AF017393] Cytochrome P450-2F4 (-3.4)
[AI233225] Guanylate cyclase β 1(-3.2)
[U90610] CXCR-4 (-3.1)
[L10669] Glycogen phosphorylase (-3.3)
[L04672] G protein coupled receptor (-3.0)
[U76032] cGMP-specific phosphodiesterase; PDE5 (-3.0)

[L09119] C kinase substrate calmodulin-binding protein RC3 (-3.0)
[AA925762] Myristoylated alanine rich protein kinase c substrate (-3.0)
[AB012234] NF1-X1 (-2.9)
[AF031384] TWIK-related acid-sensitive K⁺ channel (-2.9)
[U77697] PECAM-1 (-2.8)
[X57764] ET-B endothelin receptor (-2.8)
[U10995] Orphan receptor COUP-TFI (-2.8)
[AA997870] Regulator of G-protein signaling 3; Rgs3 (-2.8)
[AA997477] Wnt2 (-2.8)
[AI103349] SOX-18 (-2.8)

Cluster H

Genes downregulated by hyperoxia compared to room air on day 10 are as follows:

[U22424] 11 β hydroxysteroid dehydrogenase II (-11.6)
[AA818097] GLP1 receptor (-8.6)
[AA925248] Scn6a (-8.9)
[AF015304] Equilibrative nitrobenzylthioniosin-sensitive nucleoside transporter (-7.1)
[D17310] Steroid 3 α -dehydrogenase (-5.5)
[J00728] Cytochrome P450e (-5.5)
[AA819900] Protocadherin α (-5.3)
[U44845] Vitronectin (-4.9)
[AA848639] cFos-induced growth factor (-4.3)
[AA893770] Estrogen-regulated protein CBL20 (-3.4)
[K01721] Cytochrome P450-3 (-3.8)
[U97143] RET ligand 2 (-3.6)
[X63253] Serotonin transporter (-3.5)
[U76206] VTR 15-20 receptor (-3.3)
[X56596] MHC class II antigen 1 β (-3.2)
[M11251] Cytochrome P-450b (-3.2)
[M31038] MHC class I α (-3.2)
[J04591] Dipeptidyl peptidase IV (-3.2)
[M64862] Matrin F/G (-3.2)
[AA894264] EST (-3.1)
[AA875025] CRAB (-3.0)
[AA800722] EST (-3.0)
[R46974] Collagen α 1-III (-3.0)
[X79321] Tau microtubule-associated protein (-2.9)
[AI639166] EST (-2.8)
[AI177621] ICAM-2 (-2.8)

